



Research Article

Equilibria and Bogdanov-Takens Bifurcation Analysis in the Bazykin's Predator-Prey System

Shuangte Wang ^{1,2} and Hengguo Yu ¹

¹College of Mathematics and Physics, Wenzhou University, Wenzhou 325035, China

²Liushi No. 3 Middle School, Wenzhou, Zhejiang 325604, China

Correspondence should be addressed to Shuangte Wang; wanshuangte@126.com and Hengguo Yu; yuhengguo5340@163.com

Received 24 May 2022; Revised 28 July 2022; Accepted 18 August 2022; Published 22 September 2022

Academic Editor: Chunrui Zhang

Copyright © 2022 Shuangte Wang and Hengguo Yu. This is an open access article distributed under the Creative Commons Attribution License, which permits unrestricted use, distribution, and reproduction in any medium, provided the original work is properly cited.

In the paper, we proposed a Bazykin's predator-prey system to explore the equilibrium point and Bogdanov-Takens bifurcation problems. Firstly, we derived some key parameter threshold conditions to ensure that the Bazykin's predator-prey system had a multiple focus of multiplicity one, weak focus of order 2, cusps of codimension 2 and a degenerate Bogdanov-Takens singularity (focus or center case) of codimension 3. Furthermore, the distinction of two types of codimension 2 cusps was also discussed, which showed that the threshold of the two types of cusps could exhibit a cusp, which was a special case of the mentioned degenerate Bogdanov-Takens singularity (focus or center case) of codimension 3. Secondly, we systematically calculated that the Bazykin's predator-prey system could undergo two types of Bogdanov-Takens bifurcations of codimension 2 and a degenerate focus type Bogdanov-Takens bifurcation of codimension 3. Finally, some numerical examples were implemented to verify the correctness and feasibility of mathematical theory derivation, which also directly showed all possible equilibrium points and Bogdanov-Takens bifurcations of Bazykin's predator-prey system. In a word, all the research results could play an important theoretical support role in the study of controlling cyanobacteria bloom.

1. Introduction

At present and in the future, water eutrophication is still one of the major water environmental problems in the world, especially the phenomenon of cyanobacteria bloom [1]. Studying the formation mechanism of cyanobacteria bloom has important ecological and environmental significance for scientifically predicting the occurrence of cyanobacteria bloom in lakes and taking corresponding measures to reduce its impact [2]. In order to explore the formation mechanism of cyanobacteria blooms in eutrophic lakes, it is necessary to comprehensively understand the dynamic evolution process of cyanobacteria bloom and systematically analyze the synergistic influence mechanism of major factors (chemistry, physics and biology) on cyanobacteria bloom with the help of mathematical models, especially the Bazykin's predator-prey system. This is because that Bazykin's predator-prey system started from the Lotka-Volterra system,

various regulating factors were considered, such as rates of birth and death, predation and competition, these different factors can have a stabilizing or a destabilizing effect on the community, and their interplay leads to increasingly complicated behaviors, which can describe the growth dynamic mechanism of some cyanobacteria populations [3].

Bazykin [4] presented a variation of Volterra's classical predator-prey model under the help of Michaelis-Menton equation, which can be called Bazykin's predator-prey model according to Bazykin's modification. Since then, the Bazykin's predator-prey system has received the attention of a large number of scholars and obtained some excellent research results [5–10]. The paper [5] investigated bifurcations of equilibria in Bazykin's predator-prey model. The paper [6] researched stability and bifurcation of Bazykin's predator-prey model with memory effect, which can reveal the effect of memory based growth on global bifurcation threshold. The paper [7] considered Bazykin's predator-prey

model to address harvesting induced stability exchanges through bifurcation analysis, which can be useful to understand conservation policy and fishery management. The paper [8] proposed Bazykin predator-prey model with Beddington-DeAngelis response function to study persistence and global stability. The paper [9] inquired into the critical normal form coefficients and bifurcations of a discrete-time Bazykin's predator-prey model. The paper [10] theoretically and numerically studied stability and bifurcation behaviors of the Bazykin's predator-prey ecosystem with Holling type II functional response. It is obvious that the Bazykin's predator-prey system can more realistically describe the dynamic relationship between predator population and prey population, and produce relatively rich bifurcation dynamics, such as transcritical bifurcation, saddle-node bifurcation, Hopf bifurcation and Bogdanov-Takens bifurcation, which can in fact be seen as bridging the gap between mathematical biology and bifurcation theory. Furthermore, the Bazykin's predator-prey system can lead to sudden changes in ecosystem state and parameter space, which can analyze and predict qualitative changes in dynamics. Usually, these sudden changes are a very needed tool to study the outbreak of cyanobacteria bloom, because of the increasing adverse load on the cyanobacteria biosphere.

In relation to Michaelis-Menton equation, we will consider a predator-prey ordinary differential equations (ODEs) system with prey-dependent Holling type II functional response and density-dependent death rate for the predator, which is a variation of Volterra's classical predator-prey model and can be referred to Bazykin's works.

$$\begin{aligned} \dot{x} &= r_1 x \left(1 - \frac{x}{K_1}\right) - \frac{\alpha xy}{a+x} - m_1 x, \\ \dot{y} &= \frac{\alpha exy}{a+x} - m_2 y - dy^2, \end{aligned} \quad (1)$$

here the parameters r_1 , K_1 , α , a , m_1 , e , m_2 and d are all positive constants with practically biological meanings, respectively. r_1 denotes the intrinsic growth rate of the prey, K_1 represents the carrying capacity of the environment, a is the half-saturation constant, α is the search efficiency of predator for prey, m_1 and m_2 are mortality rate of the prey and predator species respectively, e is the biomass conversion, d is the intra-specific competition coefficient. The functions $x = x(t)$ and $y = y(t)$ represent densities of the prey and predator at time t , respectively. The term dy^2 represents interspecific density-restricted effect on the predator; the term $\alpha x/a+x$ (Holling type II functional response) is named after C. S. Holling, who proposed several functional responses for different kinds of species to model the phenomena of predation in 1965, since then the classical Lotka-Volterra predator-prey system in biomathematics was more advanced and realistic [11–14]. These functional responses described how predators transform harvested prey into the growth of themselves and were discussed by many researchers [15], especially the Rosenzweig-MacArthur model (R-M model) or a predator-prey model with Holling type II functional response [16].

To investigate complex dynamical behaviors of the system (1) more precisely, in this paper, we concentrate on Bogdanov-Takens (BT) bifurcations at corresponding interior equilibria, respectively. It is clear to see that all solutions of the system (1) are positive and bounded with respect to the positive initial conditions $x(0) > 0$, $y(0) > 0$. Also, the x -axis and y -axis are invariant, namely, the system (1) is dissipative in the first quadrant \mathbb{R}^{+2} and well-defined on the domain $\mathbb{R}_+^2 = \mathbb{R}^{+2}$. The rest of this paper is organized as followed. In Section 2, we mainly consider stability of interior (positive) equilibria with respect to following special cases: (i) $A_1 = 0, A_2 > 0$; (ii) $A_1 = A_2 = 0$; (iii) $A_2 = 0, A_1 \neq 0$. The first case (i) ensures the potential Hopf bifurcation with the help of standard bifurcation theory, while the second case (ii) exhibits BT bifurcations of codimension 2 with two bifurcation parameters and a degenerate focus type BT bifurcation of codimension 3 with three bifurcation parameters. The statements of bifurcations are illustrated in Section 3. Finally, we also give some numerical simulations and discussions to support our theories. The last Section 4 is a short summary.

2. Equilibria Analysis

In this section, we mainly discuss the existence conditions and stability analysis of interior equilibria in some special cases. It is clear that the system (1) has bound equilibria $E_0 = (0, 0)$, $E_1 = (0, -m_2/d)$ and $E_2 = (K_1(1 - m_1/r_1), 0)$. For biological consideration, we omit the point E_1 .

2.1. Preliminaries. In this subsection, we fully discuss preliminaries of the interior equilibrium point in the system (1). Here we denote it as $E_* = (x_*, y_*)$ for later use. An equilibrium point E_* must satisfy following algebraic polynomial form equations

$$f(x, y) = r_1 \left(1 - \frac{x}{K_1}\right) (a+x) - \alpha y - m_1 (a+x) = 0, \quad (2)$$

$$g(x, y) = \alpha ex - m_2 (a+x) - dy(a+x) = 0.$$

In other words, x_* and y_* must be positive roots of following third-order polynomials (cubic equations) $p(x) = \sum_{i=0}^3 a_i x^i$ and $p(y) = \sum_{i=0}^3 b_i y^i$, respectively, where coefficients are

$$\begin{aligned} a_3 &= dr_1, \quad a_2 = d(m_1 - r_1)K_1 + 2adr_1, \\ a_1 &= [2a(m_1 - r_1)d + \alpha(ae - m_2)]K_1 + a^2 dr_1, \\ a_0 &= [a(m_1 - r_1)d - m_2 \alpha]aK_1, \\ b_3 &= K_1 d^2, \quad b_2 = -2K_1 d(ae - m_2), \\ b_1 &= [(ae - m_2)^2 + ade(r_1 - m_1)]K_1 + a^2 der_1, \\ b_0 &= e[(m_1 - r_1)(ae - m_2)K_1 + am_2 r_1]a. \end{aligned} \quad (3)$$

We will mention an eliminant method in linear algebraic merely for completeness and shall not involve it in detail. If we sort above equations (2) as the form of $f(x, y) = a_0(x)y + a_1(x) = 0$, $g(x, y) = b_0(x)y + b_1(x) = 0$, the

cubic equation $p(x) = 0$ can also be obtained again from the first Sylvester's resultant $R_y(f, g) = a_0(x)b_1(x) - a_1(x)b_0(x)$. Similarly, if we sort the equations (2) as the form of $f(x, y) = c_0(y)x^2 + c_1(y)x + c_2(y) = 0$, $g(x, y) = d_0(y)x + d_1(y) = 0$, the second resultant

$$R_x(f, g) = \begin{vmatrix} c_0(y) & c_1(y) & c_2(y) \\ d_0(y) & d_1(y) & 0 \\ 0 & d_0(y) & d_1(y) \end{vmatrix}. \quad (4)$$

Also deduces the cubic equation $q(y) = 0$.

Thanks to Scipione del Ferro, Niccolo Fontana(Tartaglia), Gerolamo Cardano and Shengjin Fan's groundbreaking masterpieces, a third-order algebraic equation's root(s) can be formulated by Cardano's formula or Shengjin's formula, and may qualitatively have one, two or three positive roots in the light of Rene Descartes' rule of signs or Shengjin's discriminant. Here we let these complicated expressions

$$\begin{aligned} p_x &= \frac{a_1}{a_3} - \frac{1}{3} \left(\frac{a_2}{a_3} \right)^2, \\ q_x &= \frac{2}{27} \left(\frac{a_2}{a_3} \right)^3 - \frac{1}{3} \frac{a_2}{a_3} \frac{a_1}{a_3} + \frac{a_0}{a_3}, \\ \Delta_x &= \left(\frac{q_x}{2} \right)^2 + \left(\frac{p_x}{3} \right)^3, \end{aligned} \quad (5)$$

and

$$\begin{aligned} p_y &= \frac{b_1}{b_3} - \frac{1}{3} \left(\frac{b_2}{b_3} \right)^2, \\ q_y &= \frac{2}{27} \left(\frac{b_2}{b_3} \right)^3 - \frac{1}{3} \frac{b_2}{b_3} \frac{b_1}{b_3} + \frac{b_0}{b_3}, \\ \Delta_y &= \left(\frac{q_y}{2} \right)^2 + \left(\frac{p_y}{3} \right)^3, \end{aligned} \quad (6)$$

be discriminants of above cubic equations $p(x) = 0$ and $q(y) = 0$, respectively [5].

The interior equilibrium point E_* does not exist when $r_1 \leq m_1$ or $ae \leq m_2$, thus we always assume $r_1 > m_1$ and $ae > m_2$ in the rest of this paper. The isoclines from the equations (2) and cobweb model show that an interior equilibrium point E_* exists if condition

$$0 < \frac{m_2 a}{ae - m_2} < K_1 \left(1 - \frac{m_1}{r_1} \right), \quad (7)$$

holds. Noticing that the condition (7) deduces $a_0 < 0, b_0 < 0$, according to the zero theorem and

$$p \left(\frac{m_2 a}{ae - m_2} \right) = \frac{[-ae x_2 + m_2(a + x_2)]e^2 r_1 a^2 \alpha^2 d}{(ae - m_2)^3} < 0, \quad (8)$$

$$q \left(\frac{ae - m_2}{d} \right) = a^2 \alpha^2 r_1 > 0.$$

It is supposed that such condition (7) is well-done. In addition, the condition (7) and one of following conditions

$$\begin{aligned} (i) & \frac{x_2 - a}{2} \leq \frac{m_2 a}{ae - m_2}, \\ (ii) & a_1, a_2 \geq 0, \\ (iii) & a_2^2 - 3a_1 a_3 \leq 0, \\ (iv) & b_2^2 - 3b_1 b_3 \leq 0, \end{aligned} \quad (9)$$

can lead to the uniqueness of the equilibrium point E_* , here $x_2 = K_1(1 - (m_1/r_1))$.

2.2. Multiple Focus with Multiplicity One. Due to the Routh-Hurwitz criterion and the Perron's theorems, we merely need to consider the Jacobian matrix at a non-hyperbolic interior equilibrium point E_* :

$$\begin{aligned} J(E_*) &= (J_{ij})_{2 \times 2} \\ &= \begin{bmatrix} \frac{\alpha x_* y_*}{(a + x_*)^2} - \frac{r_1 x_*}{K_1} - \frac{\alpha x_*}{a + x_*} & \\ \frac{\alpha e a y_*}{(a + x_*)^2} & -d y_* \end{bmatrix}. \end{aligned} \quad (10)$$

Furthermore, the trace, determinant and discriminant of matrix $J(E_*)$ are denoted as

$$\begin{aligned} A_1 &:= A_1(E_*) \\ &= \text{tr}J(E_*) \\ &= \frac{-2r_1 x_*^2 + [(-ae - m_1 + m_2 + r_1)K_1 - r_1 a]x_* + K_1 a m_2}{K_1(a + x_*)}, \end{aligned} \quad (11)$$

$A_2 := A_2(E_*) = \det J(E_*)$ and $\Delta_* := \Delta_*(E_*) = A_1^2 - 4A_2$, respectively. In order to obtain potential Hopf bifurcation, i.e. $A_1 = 0$ and $A_2 > 0$ (matrix $J(E_*)$ has a pair of pure imaginary eigenvalues), we take the threshold of parameter $m_1 = r_1 - ae - m_2$, which can ensure that the numerator of A_1 has a perfect square discriminant with respect of variable x_* . Thus the system (1) has an equilibrium point $E_3 := (x_3, y_3) = (a\lambda\mu, (\lambda\mu + 1)ea)$ with parameters

$$\begin{aligned} m_2 &= \lambda a e, \\ K_1 &= \frac{\mu a r_1}{ae}, \end{aligned} \quad (12)$$

$$d = \frac{\alpha[(\lambda - 1)\mu + 1]\lambda}{a(\lambda\mu + 1)^2},$$

and control variables $\lambda \in (0, 1), \mu > \mu_m = 1/1 - \lambda$. This special case is now denoted as (C1) for later use.

Let us firstly discuss the equilibrium E_3 more qualitatively, under the assumption of this case, the determinant is simplified as

$$A_2(E_3) = \frac{\lambda \alpha^2 e^2 \varphi_{A_2}(\lambda, \mu)}{(\lambda \mu + 1)^2}, \quad (13)$$

$$\varphi_{A_2}(\lambda, \mu) = \lambda^3 \mu^2 + (-2\mu^2 + 2\mu)\lambda^2 + (\mu - 1)^2 \lambda - \mu.$$

The equation $\varphi_{A_2}(\lambda, \mu) = 0$ has a quite clear positive root.

$$\mu_1 = \frac{-2\lambda^2 + 2\lambda + 1 + s}{2\lambda(1 - \lambda)^2} > \mu_m, \quad (14)$$

$$s = \sqrt{-4\lambda^2 + 4\lambda + 1}.$$

That is to say: (i) $A_2(E_3) > 0$ and E_3 is a center or focus when $\mu \in (\mu_m, \mu_1)$; (ii) $A_2(E_3) = 0$ and E_3 is a potential cusp of codimension at least 2 when $\mu = \mu_1$; (iii) $A_2(E_3) < 0$ and E_3 is just a saddle point when $\mu > \mu_1$.

This subsection will deal with above case (i). By using transformation $x = u + x_3$, $y = v + y_3$, the point E_3 is translated to the origin $O = (0, 0)$. Making a change of variables as $u = -d y_3 X + \beta Y$, $v = -a e a y_3 / (a + x_3)^2 X$, in which $\beta = \sqrt{A_2(E_3)} > 0$, then the system (1) becomes

$$\dot{X} = F_2(X, Y) = -\beta Y + \sum_{i+j=2}^3 a_{ij} X^i Y^j + O(|X, Y|^4), \quad (15)$$

$$\dot{Y} = G_2(X, Y) = \beta X + \sum_{i+j=2}^3 b_{ij} X^i Y^j + O(|X, Y|^4).$$

Following [17, 18], the first Lyapunov number of the system (15) at the point E_3 , which is used to determine the stability of limit cycles as well, is presented as.

$$\begin{aligned} \sigma &= \frac{3\pi}{2\beta} \left\{ 3(a_{30} + b_{03}) + (a_{12} + b_{21}) \right. \\ &\quad \left. - \frac{1}{\beta} [2(a_{20}b_{20} - a_{02}b_{02}) - a_{11}(a_{02} + a_{20}) + b_{11}(b_{02} + b_{20})] \right\} \\ &= \frac{3\pi \alpha^3 e^3 \lambda \mu \varphi_\sigma(\lambda, \mu)}{2a^2(\lambda \mu + 1)^4 \beta \varphi_{A_2}(\lambda, \mu)}, \end{aligned} \quad (16)$$

where

$$\varphi_\sigma(\lambda, \mu) = 2 + 2\lambda^4 \mu^2 + (4\mu - 2\mu^2)\lambda^3 + (2 - \mu)\lambda^2 + (\mu + 1)\lambda. \quad (17)$$

The transformation $u = \beta X + d y_3 Y$, $v = a e a y_3 / (a + x_3)^2 Y$ can also be used to deduce σ in (16).

For any arbitrary λ , in view of a quadratic function $\varphi_\sigma(\lambda, \mu)$ with respect to variable μ , it is a downward opening parabola with a symmetry axis $\mu = 4\lambda^2 - \lambda + 1/4\lambda^2(1 - \lambda) > 0$ and has a positive maximum $\lambda^2 + 14\lambda + 1/8\lambda(1 - \lambda)$. The equation $\varphi_\sigma(\lambda, \mu) = 0$ straightly has a unique positive root

$$\mu_\sigma = \frac{4\lambda^2 + \sqrt{\lambda^2 + 14\lambda + 1 - \lambda + 1}}{4\lambda^2(1 - \lambda)} > \mu_m. \quad (18)$$

What is more, $\mu_1 > \mu_\sigma$ (or μ_σ exists) if $\lambda > 2/5$; $\mu_1 < \mu_\sigma$ if $\lambda < 2/5$; $\mu_1 = \mu_\sigma$ only if $\lambda = 2/5$. Therefore, the equilibrium point E_3 is respectively a stable(unstable if μ_σ exists) multiple

focus with multiplicity one if $\mu < \mu_\sigma$ ($> r b i n \mu_\sigma$). When $\mu = \mu_\sigma$ (if μ_σ exists), σ vanishes and one need to calculate the second Lyapunov coefficient l_2 . The generalized Hopf bifurcation of codimension 2 (Bautin bifurcation) may occur and two homocentric limit cycles may appear in some particular cases around the Bautin point E_3 if $l_2 \neq 0$.

2.3. Weak Focus of Order 2. When $\mu = \mu_\sigma$, the first Lyapunov coefficient will be zero and we need to treat a weak (fine) focus E_3 of order at least 2 in the so-called center-focus problem. This subsection starts with the system (15) or a standard form

$$\begin{aligned} \dot{x} &= -\beta y + \varphi(x, y), \\ \dot{y} &= \beta x + \psi(x, y), \end{aligned} \quad (19)$$

where $\varphi(x, y)$, $\psi(x, y)$ are both analytical functions and $\varphi(0, 0) = \psi(0, 0) = 0$. Taking the polar coordinate transformation $x = r \cos \theta$, $y = r \sin \theta$, we derive a new system $\dot{r} = rR(r, \theta)$, $\dot{\theta} = \beta + Q(r, \theta)$, where $R(r, \theta) = \varphi \cos \theta + \psi \sin \theta$, $Q(r, \theta) = 1/r(\psi \cos \theta - \varphi \sin \theta)$ are also analytical functions. Now we rewrite the above system as

$$\frac{dr}{d\theta} = \frac{rR}{\beta + Q} = \sum_{k=2}^{\infty} R_k(\theta) r^k, \quad (20)$$

here $R_k(\theta)$ are just polynomials of triangle functions $\cos \theta$ and $\sin \theta$.

We suppose that the special solution of the system (20) with initial condition $r(\theta = 0) = c$ is $r(\theta, c) = \sum_{k=1}^{\infty} r_k(\theta) c^k$. Substituting it into the equation (20) and comparing all terms in c^k , we have a series of coupled first-order differential equations

$$\frac{dr_1}{d\theta} = 0, \frac{dr_2}{d\theta} = R_2 r_1^2, \frac{dr_3}{d\theta} = 2R_2 r_1 r_2 + R_3 r_1^3, \dots \quad (21)$$

These equations naturally yield solutions $r_1 = 1$, $r_k = g_k \theta + \varphi_k(\theta)$ ($k > 1$), where involved constants are

$$g_2 = \frac{1}{2\pi} \int_0^{2\pi} R_2(\tau) d\tau, g_3 = \frac{1}{2\pi} \int_0^{2\pi} [R_3(\tau) + 2R_2(\tau)r_2(\tau)] d\tau, \quad (22)$$

and $\varphi_k(\theta)$ are periodic functions with a period 2π as well. For the system (19) with standard form, we obviously derive the first focal quantity g_3 with $g_2 = 0$, which repeats the formula (16) again, i.e. $g_3/\sigma \equiv \text{constant} > 0$.

If $g_3 = 0$ or $\sigma = 0$, from the integrals (22), we know $g_4 = 0$ and the second focal quantity g_5 (see the Appendix). From now on, with the system (15) at hand, the second focal quantity g_5 reads

$$g_5 = -\frac{2097152\lambda^8 e^4 \alpha^4 \sqrt{2}(\lambda - 1)^6 \varphi_{g_5}(\lambda)}{3a^4(s_1 + 3\lambda + 1)^{12} (4\lambda^2 - \lambda + s_1 + 1)^4 \sqrt{1 - \lambda} \psi_{g_5}(\lambda)^{7/2}}, \quad (23)$$

in which auxiliary functions are $\psi_{g_5}(\lambda) = 9\lambda^3 - \lambda^2 s_1 + 3\lambda^2 + 4\lambda s_1 - 3\lambda - s_1 - 1$ and

$$\begin{aligned}
 \varphi_{g_5}(\lambda) = & 1 + s_1 + (54s_1 + 61)\lambda + (1179s_1 + 1533)\lambda^2 + (13252s_1 + 20377)\lambda^3 \\
 & + (79878s_1 + 151954)\lambda^4 + (230064s_1 + 604458)\lambda^5 + (57696s_1 + 873264)\lambda^6 \\
 & + (-1682544s_1 - 2369616)\lambda^7 + (-6203262s_1 - 14628750)\lambda^8 \\
 & + (-11558132s_1 - 36469478)\lambda^9 + (-6708162s_1 - 43299230)\lambda^{10} \\
 & + (22132104s_1 + 19510890)\lambda^{11} + (88954156s_1 + 206053636)\lambda^{12} \\
 & + (179705232s_1 + 536172580)\lambda^{13} + (268668984s_1 + 899927400)\lambda^{14} \\
 & + (310805040s_1 + 1188987000)\lambda^{15} + (295112037s_1 + 1226575797)\lambda^{16} \\
 & + (224630382s_1 + 1060506033)\lambda^{17} + (141939919s_1 + 727205209)\lambda^{18} \\
 & + (69055348s_1 + 415540245)\lambda^{19} + (27134470s_1 + 180678370)\lambda^{20} \\
 & + (6942224s_1 + 61201034)\lambda^{21} + (1283776s_1 + 13517744)\lambda^{22} \\
 & + (19840s_1 + 1703872)\lambda^{23} + (-800s_1 - 14240)\lambda^{24} + 800\lambda^{25}.
 \end{aligned} \tag{24}$$

Symbol s_1 is $\sqrt{\lambda^2 + 14\lambda + 1}$. The resultant

$$\begin{aligned}
 R_{s_1}(\varphi_{g_5}) = & 1048576(5\lambda - 2)^2\lambda^{17}(\lambda - 1)^{14}(12\lambda^3 + 2\lambda^2 + 2\lambda - 1) \\
 & \cdot (\lambda^2 + 2\lambda + 3)^2(2\lambda^2 + \lambda + 2)^4 \neq 0.
 \end{aligned} \tag{25}$$

Implies that $\varphi_{g_5}(\lambda) > 0$ when $\lambda \in (2/5, 1)$. While $\psi_{g_5}(\lambda)$ is also positive since $R_{s_1}(\psi_{g_5}) = 16\lambda^2(\lambda - 1)(5\lambda - 2)(\lambda^2 + 2\lambda + 3) \neq 0$, then $g_5 < 0 (\neq 0)$. In other words, the equilibrium point E_3 with $\sigma = 0$ is a stable weak focus of order 2.

2.4. Cusp of Codimension 2. From the case (C1), undaunted by the scale of the distinction, this subsection reasonably set about finishing a puzzle when $\mu = \mu_1$. Letting $A_2 = 0$ in this case, we have threshold of parameters, a nilpotent $E_*^{(2)} = (x_*^{(2)}, y_*^{(2)})$ and an elementary equilibrium $E_*^{(1)} = (x_*^{(1)}, y_*^{(1)})$ as follows:

$$\begin{aligned}
 m_1 = r_1 - (\lambda + 1)ae, d = & \frac{\lambda\alpha(\mu_1 - \lambda\mu_1 - 1)}{a(\lambda\mu_1 + 1)^2}, \\
 x_*^{(2)} = \mu_1 a\lambda, y_*^{(2)} = & ea(\lambda\mu_1 + 1), \\
 x_*^{(1)} = \frac{[(\lambda^2 - \lambda + 1)s - \lambda^2 + \lambda + 1]a}{\lambda(s + 1)(\lambda - 1)}, & \tag{26} \\
 y_*^{(1)} = \frac{2ae(s\lambda + 2\lambda^2 - 2s - \lambda - 2)}{(\lambda - 1)(-2\lambda^2 + 2\lambda + 1 + s)}. &
 \end{aligned}$$

Firstly, we can make a transformation (I): $x = X + x_*^{(2)}$, $y = Y + y_*^{(2)}$ for the system (1) with above threshold of parameters:

$$\dot{X} = F_1(X, Y), \dot{Y} = G_1(X, Y). \tag{27}$$

Secondly, we take the transformation

$$\text{(II): } X = \frac{1}{4}(s - 2\lambda + 1)aeu + v, Y = \frac{ae^2(s - 2\lambda + 1)(s - 1)u}{8\lambda}. \tag{28}$$

Thus above system becomes Jordan's standard form

$$\begin{aligned}
 \dot{u} = F_2(u, v) = v + a_{20}u^2 + a_{11}uv + a_{02}v^2 + O(|u, v|^3), \\
 \dot{v} = G_2(u, v) = b_{20}u^2 + b_{11}uv + b_{02}v^2 + O(|u, v|^3).
 \end{aligned} \tag{29}$$

By using the Lemma 1 (or the Lemma 1 in [19]), this system (29) is equivalent to following system

$$\begin{aligned}
 \dot{x} = y, \\
 \dot{y} = d_1(\lambda)x^2 + d_2(\lambda)xy + O(|x, y|^3),
 \end{aligned} \tag{30}$$

where discriminants manipulated by λ are

$$\begin{aligned}
 d_1 = d_1(\lambda) = b_{20} = \frac{\alpha^3 e^3 (\lambda - 1)^4 \varphi_{d_1}(\lambda)}{4a(2\lambda s + 4\lambda - 3s - 5)}, \\
 d_2 = d_2(\lambda) = b_{11} + 2a_{20} \\
 = \frac{\alpha^2 e^2 \lambda (1 - \lambda)^3 [s^3 + (5 - 2\lambda)s^2 + (19 - 12\lambda)s + 23 - 18\lambda]}{a(s + 1)\psi_{d_2}(\lambda)}.
 \end{aligned} \tag{31}$$

Here temporarily auxiliary functions are $\varphi_{d_1}(\lambda) = 2\lambda s - 2s^2 + 8\lambda - s + 1$ and $\psi_{d_2}(\lambda) = s^3 + (2\lambda - 1)s^2 + (12\lambda - 15)s + 14\lambda - 17$. We have added control variable $s \in (1, \sqrt{2}]$.

Lemma 1. The following system

$$\begin{aligned}
 \dot{x} = y + Ax^2 + Bxy + Cy^2 + O(|x, y|^3), \\
 \dot{y} = Dx^2 + Exy + Fy^2 + O(|x, y|^3),
 \end{aligned} \tag{32}$$

is equivalent to the system

$$\begin{aligned}
 \dot{x} = y, \\
 \dot{y} = Dx^2 + (E + 2A)xy + O(|x, y|^3).
 \end{aligned} \tag{33}$$

After some nonsingular transformations in the neighbourhood of the origin O .

Letting function $\varphi_{d_1}(\lambda)$ be zero and solving out the threshold of λ from the resultant (determinant)

$$R_s(\varphi_{d_1}) = \begin{vmatrix} 1 & \frac{1-2\lambda}{2} & \frac{-1-8\lambda}{2} & 0 \\ 0 & 1 & \frac{1-2\lambda}{2} & \frac{-1-8\lambda}{2} \\ 1 & 0 & h(\lambda) & 0 \\ 0 & 1 & 0 & h(\lambda) \end{vmatrix} = 4\lambda^3(5\lambda - 2), \quad (34)$$

or equation $\varphi_{d_1}(\lambda) = 0$, it leads to a unique solution $\lambda = 2/5$, where $h(\lambda) = 4\lambda^2 - 4\lambda - 1$. And the derivative

$$\frac{d\varphi_{d_1}(\lambda)}{d\lambda} = \frac{2}{s} [(s^2 - 1) + 8s\lambda + 4\lambda(1 - \lambda)] > 0. \quad (35)$$

Implies that the function $\varphi_{d_1}(\lambda)$ is a monotonic increasing function defined on interval $(0, 1)$. Combining the denominator of d_1 :

$$4a(2\lambda s + 4\lambda - 3s - 5) = 4a[(2s + 4)(\lambda - 1) - (s + 1)] < 0. \quad (36)$$

Here we know that $d_1 < (>)0$ if $\lambda > (<)2/5$. Notice that the numerator of d_2 is obviously positive since the range of λ . In fact, we can assert that d_2 is non zero. Indeed, for the function $\psi_{d_2}(\lambda)$ in the denominator of d_2 , its negativity will be found and well verified from an inequality

$$\psi_{d_2}(\lambda) = s^2(s + \lambda) - 3(s + 1) + (\lambda - 1)(s^2 + 12s + 14) < (s^2 - 3)(s + 1). \quad (37)$$

That is to say, $\psi_{d_2}(\lambda)$ is always negative, namely d_2 is negative here. All in all, $d_1 d_2 \neq 0$ when $m_2 \neq 2/5ae$, while $d_1 d_2 = 0$ when $m_2 = 2/5ae$.

Next, we mainly concentrate on the stability of the equilibrium point $E_*^{(1)}$ whose trace, determinant and discriminant are parameterized as

$$\begin{aligned} A_1(E_*^{(1)}) &= \frac{\alpha e(5-s)\varphi_{A_1}(\lambda)}{2(s+1)(2\lambda s + 4\lambda - 3s - 5)}, \\ A_2(E_*^{(1)}) &= \frac{\alpha e(\alpha e - m_2)(s-3)\varphi_{A_2}(\lambda)}{2(s+1)(2\lambda s + 4\lambda - 3s - 5)}, \\ \Delta_*(E_*^{(1)}) &= -\frac{m_2^2 \varphi_{\Delta}(\lambda)}{(s+1)^4 \psi_{\Delta}(\lambda)}. \end{aligned} \quad (38)$$

In which some continuous auxiliary functions can be respectively expressed by

$$\begin{aligned} \varphi_{A_1}(\lambda) &= -2s^3 + (2\lambda - 7)s^2 + (-6\lambda + 6)s - 16\lambda + 19, \\ \varphi_{A_2}(\lambda) &= s^3 + (14\lambda - 19)s^2 + (12\lambda - 9)s - 34\lambda + 43, \\ \varphi_{\Delta}(\lambda) &= \sum_{j=1}^9 x_j s^{9-j}, \\ \psi_{\Delta}(\lambda) &= s^4 + 4s^3 + (8\lambda - 6)s^2 + (28\lambda - 34)s + 24\lambda - 29, \end{aligned} \quad (39)$$

with

$$\begin{aligned} x_1 &= 1, x_2 = 64\lambda - 226, x_3 = 124\lambda - 354, x_4 = -1532\lambda + 3156, \\ x_5 &= -2452\lambda + 5010, x_6 = 8248\lambda - 11682, x_7 = 13172\lambda - 18786, \\ x_8 &= -10108\lambda + 12208, x_9 = -16476\lambda + 19889. \end{aligned} \quad (40)$$

The determinants

$$\begin{aligned} R_s(\varphi_{A_1}) &= \begin{vmatrix} 1 & -\lambda + \frac{7}{2} & 3\lambda - 3 & 8\lambda - \frac{19}{2} & 0 \\ 0 & 1 & -\lambda + \frac{7}{2} & 3\lambda - 3 & 8\lambda - \frac{19}{2} \\ 1 & 0 & h(\lambda) & 0 & 0 \\ 0 & 1 & 0 & h(\lambda) & 0 \\ 0 & 0 & 1 & 0 & h(\lambda) \end{vmatrix} \\ &= 16(5\lambda - 2)(\lambda - 1)^5, \\ R_s(\varphi_{A_2}) &= \begin{vmatrix} 1 & 14\lambda - 19 & 12\lambda - 9 & -34\lambda + 43 & 0 \\ 0 & 1 & 14\lambda - 19 & 12\lambda - 9 & -34\lambda + 43 \\ 1 & 0 & h(\lambda) & 0 & 0 \\ 0 & 1 & 0 & h(\lambda) & 0 \\ 0 & 0 & 1 & 0 & h(\lambda) \end{vmatrix} \\ &= 128(5\lambda - 2)^2(\lambda - 1)^4, \end{aligned} \quad (41)$$

and

$$\begin{aligned} R_s(\varphi_{\Delta}) &= \begin{vmatrix} 1 & x_2 & x_3 & x_4 & x_5 & x_6 & x_7 & x_8 & x_9 & 0 \\ 0 & 1 & x_2 & x_3 & x_4 & x_5 & x_6 & x_7 & x_8 & x_9 \\ 1 & 0 & h(\lambda) & 0 & 0 & 0 & 0 & 0 & 0 & 0 \\ 0 & 1 & 0 & h(\lambda) & 0 & 0 & 0 & 0 & 0 & 0 \\ 0 & 0 & 1 & 0 & h(\lambda) & 0 & 0 & 0 & 0 & 0 \\ 0 & 0 & 0 & 1 & 0 & h(\lambda) & 0 & 0 & 0 & 0 \\ 0 & 0 & 0 & 0 & 1 & 0 & h(\lambda) & 0 & 0 & 0 \\ 0 & 0 & 0 & 0 & 0 & 1 & 0 & h(\lambda) & 0 & 0 \\ 0 & 0 & 0 & 0 & 0 & 0 & 1 & 0 & h(\lambda) & 0 \\ 0 & 0 & 0 & 0 & 0 & 0 & 0 & 1 & 0 & h(\lambda) \end{vmatrix} \\ &= 65536(41\lambda^2 - 54\lambda + 81)(\lambda - 1)^{12}(5\lambda - 2)^2, \end{aligned} \quad (42)$$

which are respectively from equations $\varphi_{A_1}(\lambda) = 0$, $\varphi_{A_2}(\lambda) = 0$ and $\varphi_{\Delta}(\lambda) = 0$, yield the unique solution (zero point) $\lambda = 2/5$ once more.

For the sake of mathematical natures of the functions $\varphi_{A_1}(\lambda)$, $\varphi_{A_2}(\lambda)$, $\varphi_{\Delta}(\lambda)$ and $\psi_{\Delta}(\lambda)$ defined on interval $(0, 1)$, we calculate their derivatives up to second order with respect to λ :

$$\begin{aligned} \frac{d\varphi_{A_1}(\lambda)}{d\lambda} &= \frac{\varphi_{D\varphi_{A_1}}(\lambda)}{s}, \\ \frac{d^2\varphi_{A_1}(\lambda)}{d\lambda^2} &= \frac{24s^4 + (-48\lambda + 72)s^3 + (-96\lambda^2 + 168\lambda - 72)s^2 + 96(\lambda - 1)(\lambda - 1/2)^2}{s^3}, \\ \frac{d\varphi_{A_2}(\lambda)}{d\lambda} &= \frac{\varphi_{D\varphi_{A_2}}(\lambda)}{s}, \\ \frac{d^2\varphi_{A_2}(\lambda)}{d\lambda^2} &= \frac{-12s^4 + (-336\lambda + 264)s^3 + (48\lambda^2 - 192\lambda + 96)s^2 - 192\lambda^3 + 336\lambda^2 - 192\lambda + 36}{s^3}, \\ \frac{d\varphi_{\Delta}(\lambda)}{d\lambda} &= \frac{\varphi_{D\varphi_{\Delta}}(\lambda)}{s}, \\ \frac{d^2\varphi_{\Delta}(\lambda)}{d\lambda^2} &= \frac{1}{s^3} \left[-32s^9 + (-5376\lambda + 8120)s^8 + (768\lambda^2 - 9696\lambda + 11664)s^7 \right. \\ &\quad + (35840\lambda^3 - 162400\lambda^2 + 227440\lambda - 125400)s^6 \\ &\quad + (47616\lambda^3 - 183552\lambda^2 + 265536\lambda - 153376)s^5 \\ &\quad + (-367680\lambda^3 + 1125120\lambda^2 - 1146288\lambda + 428520)s^4 \\ &\quad + (-313856\lambda^3 + 955136\lambda^2 - 1035872\lambda + 415984)s^3 \\ &\quad + (395904\lambda^3 - 956640\lambda^2 + 781008\lambda - 229448)s^2 \\ &\quad \left. + 161728\left(\lambda - \frac{1}{2}\right)^2\left(\lambda - \frac{436}{361}\right) \right], \\ \frac{d\psi_{\Delta}(\lambda)}{d\lambda} &= \frac{\varphi_{D\psi_{\Delta}}(\lambda)}{s}, \end{aligned} \tag{43}$$

where new auxiliary continuous functions are

$$\begin{aligned} \varphi_{D\varphi_{A_1}}(\lambda) &= 2s^3 + (24\lambda - 18)s^2 + (-16\lambda^2 + 64\lambda - 44)s + 24\lambda^2 - 36\lambda + 12, \\ \varphi_{D\varphi_{A_2}}(\lambda) &= 14s^3 + (-12\lambda + 18)s^2 + (-112\lambda^2 + 208\lambda - 110)s - 48\lambda^2 + 60\lambda - 18, \\ \varphi_{D\varphi_{\Delta}}(\lambda) &= 64 \sum_{j=1}^9 y_j s^{9-j}, \\ \varphi_{D\psi_{\Delta}}(\lambda) &= (-16\lambda + 16)s^3 + (-48\lambda + 52)s^2 + (-64\lambda^2 + 80\lambda)s - 112\lambda^2 + 192\lambda - 68, \end{aligned} \tag{44}$$

in which

$$\begin{aligned}
y_1 &= 1, y_2 = \frac{-32\lambda + 140}{64}, y_3 = \frac{-1792\lambda^2 + 7224\lambda - 4696}{64}, \\
y_4 &= \frac{-2976\lambda^2 + 9984\lambda - 6700}{64}, y_5 = \frac{30640\lambda^2 - 78440\lambda + 39808}{64}, \\
y_6 &= \frac{39232\lambda^2 - 99776\lambda + 53252}{64}, y_7 = \frac{-98976\lambda^2 + 189672\lambda - 80200}{64}, \\
y_8 &= \frac{-105376\lambda^2 + 202976\lambda - 91620}{64}, y_9 = \frac{40432\lambda^2 - 69048\lambda + 24416}{64}.
\end{aligned} \tag{45}$$

The following determinants

$$\begin{aligned}
R_s(\varphi_{D\varphi_{A_1}}) &= \begin{vmatrix} 1 & 12\lambda - 9 & -8\lambda^2 + 32\lambda - 22 & 12\lambda^2 - 18\lambda + 6 & 0 \\ 0 & 1 & 12\lambda - 9 & -8\lambda^2 + 32\lambda - 22 & 12\lambda^2 - 18\lambda + 6 \\ 1 & 0 & h(\lambda) & 0 & 0 \\ 0 & 1 & 0 & h(\lambda) & 0 \\ 0 & 0 & 1 & 0 & h(\lambda) \end{vmatrix} \\
&= 144(\lambda - 1)^4(20\lambda^2 - 12\lambda - 3), \\
R_s(\varphi_{D\varphi_{A_2}}) &= \begin{vmatrix} 1 & \frac{-6\lambda + 9}{7} & -8\lambda^2 + \frac{104\lambda - 55}{7} & \frac{-24\lambda^2 + 30\lambda - 9}{7} & 0 \\ 0 & 1 & \frac{-6\lambda + 9}{7} & -8\lambda^2 + \frac{104\lambda - 55}{7} & \frac{-24\lambda^2 + 30\lambda - 9}{7} \\ 1 & 0 & h(\lambda) & 0 & 0 \\ 0 & 1 & 0 & h(\lambda) & 0 \\ 0 & 0 & 1 & 0 & h(\lambda) \end{vmatrix} \\
&= \frac{1152}{49}(5\lambda - 2)(5\lambda + 1)(\lambda - 1)^4, \\
R_s(\varphi_{D\varphi_{\Delta}}) &= \begin{vmatrix} 1 & y_2 & y_3 & y_4 & y_5 & y_6 & y_7 & y_8 & y_9 & 0 \\ 0 & 1 & y_2 & y_3 & y_4 & y_5 & y_6 & y_7 & y_8 & y_9 \\ 1 & 0 & h(\lambda) & 0 & 0 & 0 & 0 & 0 & 0 & 0 \\ 0 & 1 & 0 & h(\lambda) & 0 & 0 & 0 & 0 & 0 & 0 \\ 0 & 0 & 1 & 0 & h(\lambda) & 0 & 0 & 0 & 0 & 0 \\ 0 & 0 & 0 & 1 & 0 & h(\lambda) & 0 & 0 & 0 & 0 \\ 0 & 0 & 0 & 0 & 1 & 0 & h(\lambda) & 0 & 0 & 0 \\ 0 & 0 & 0 & 0 & 0 & 1 & 0 & h(\lambda) & 0 & 0 \\ 0 & 0 & 0 & 0 & 0 & 0 & 1 & 0 & h(\lambda) & 0 \\ 0 & 0 & 0 & 0 & 0 & 0 & 0 & 1 & 0 & h(\lambda) \end{vmatrix} \\
&= 128(6560\lambda^4 - 12808\lambda^3 + 14305\lambda^2 - 4395\lambda - 1520)(5\lambda - 2)(\lambda - 1)^{11},
\end{aligned} \tag{46}$$

and

$$R_s(\varphi_{D\psi_\Delta}) = \begin{vmatrix} 1 & \frac{-48\lambda + 52}{-16\lambda + 16} & \frac{-64\lambda^2 + 80\lambda}{-16\lambda + 16} & \frac{-112\lambda^2 + 192\lambda - 68}{-16\lambda + 16} & 0 \\ 0 & 1 & \frac{-48\lambda + 52}{-16\lambda + 16} & \frac{-64\lambda^2 + 80\lambda}{-16\lambda + 16} & \frac{-112\lambda^2 + 192\lambda - 68}{-16\lambda + 16} \\ 1 & 0 & h(\lambda) & 0 & 0 \\ 0 & 1 & 0 & h(\lambda) & 0 \\ 0 & 0 & 1 & 0 & h(\lambda) \end{vmatrix} = 64\lambda(\lambda - 1)^5, \quad (47)$$

which are respectively constructed from equations $\varphi_{D\varphi_{A_1}}(\lambda) = 0$, $\varphi_{D\varphi_{A_2}}(\lambda) = 0$, $\varphi_{D\varphi_\Delta}(\lambda) = 0$ and $\varphi_{D\psi_\Delta}(\lambda) = 0$, yield that:

- (i) The function $\varphi_{A_1}(\lambda)$ has a (local) minimum $\varphi_{A_1}(3 + 2\sqrt{6}/10) = 227 - 147\sqrt{6}/25$ on interval $[0, 1]$ since $d^2/d\lambda^2 \varphi_{A_1}(3 + 2\sqrt{6}/10) = 438\sqrt{6} - 1008 > 0$, and, the detailed numerical simulation results are shown in Figure 1(a);
- (ii) The function $\varphi_{A_2}(\lambda)$ has a (local) minimum $\varphi_{A_2}(2/5) = 0$ on interval $[0, 1]$ since $d^2/d\lambda^2 \varphi_{A_2}(2/5) = 6480/49 > 0$, and, the detailed

numerical simulation results are shown in Figure 1(b);

- (iii) The function $\varphi_\Delta(\lambda)$ has a local minimum $\varphi_\Delta(2/5) = 0$ and a local maximum $\varphi_\Delta(\lambda_3) \approx 534.507461$ on interval $[0, 1]$ since $d^2/d\lambda^2 \varphi_\Delta(2/5) = 1156415616/30625 > 0$ and $d^2/d\lambda^2 \varphi_\Delta(\lambda_3) \approx -13531.790941 < 0$, where λ_3 is another positive root of equation $\varphi_{D\varphi_\Delta}(\lambda) = 0$ or the unique positive root of equation $6560\lambda^4 - 12808\lambda^3 + 14305\lambda^2 - 4395\lambda - 1520 = 0$ in open interval $(0, 1)$, i.e.

$$\lambda_3 = \frac{1}{9840M^{1/6}N^{1/4}} \left\{ \sqrt{6} \left[\begin{array}{l} -205\sqrt{N}M^{2/3} + (-4040497M^{1/3} + 17198445275)\sqrt{N} \\ +6993186747\sqrt{3M} \end{array} \right]^{1/2} + 4803M^{1/6}N^{1/4} - \sqrt{3}N^{3/4} \right\} \approx 0.764691, \quad (48)$$

with

$$\begin{aligned} M &= 2783067866245 + 19175820\sqrt{22669769211}, \\ N &= 410M^{2/3} - 4040497M^{1/3} - 34396890550, \end{aligned} \quad (49)$$

and then, the detailed numerical simulation results are shown in Figure 1(c); (iv) The function $\psi_\Delta(\lambda)$ is a monotonic function on interval $(0, 1)$ since $d\psi_\Delta(\lambda)/d\lambda \neq 0$, and, the detailed numerical simulation results are shown in Figure 1(d).

Hence, maxima and minima of the functions $\varphi_{A_1}(\lambda)$, $\varphi_{A_2}(\lambda)$, $\varphi_\Delta(\lambda)$ and $\psi_\Delta(\lambda)$ on unit interval $[0, 1]$ are listed as follows:

$$\begin{aligned} \max\{\varphi_{A_1}(\lambda)\} &= 16, \min\{\varphi_{A_1}(\lambda)\} = \frac{227 - 147\sqrt{6}}{25} < 0, \\ \max\{\varphi_{A_2}(\lambda)\} &= 16, \min\{\varphi_{A_2}(\lambda)\} = 0, \\ \max\{\varphi_\Delta(\lambda)\} &= 9216, \min\{\varphi_\Delta(\lambda)\} = 0, \\ \max\{\psi_\Delta(\lambda)\} &= -4, \min\{\psi_\Delta(\lambda)\} = -64. \end{aligned} \quad (50)$$

Combining Figures 1(a)–1(d) and the determinant

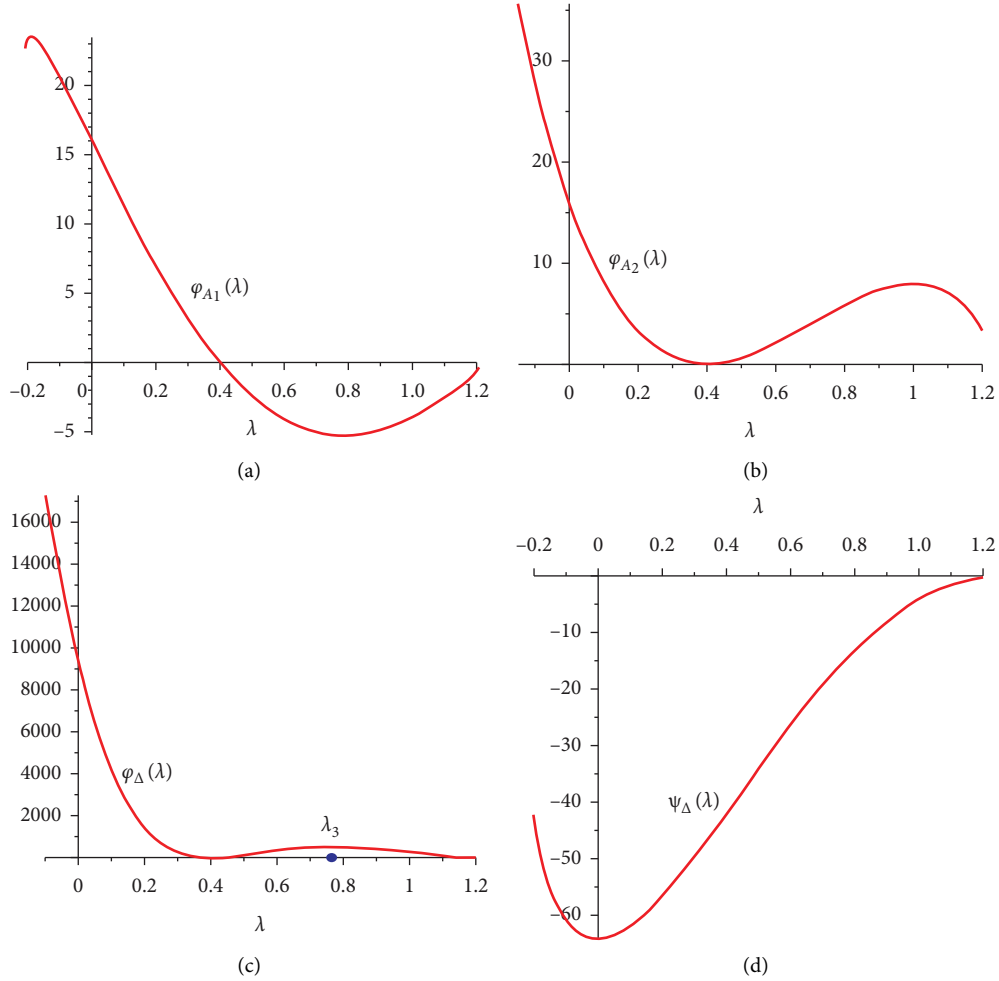


FIGURE 1: (a) Figure of function $\varphi_{A_1}(\lambda)$ on the interval $[0, 1]$; (b) figure of function $\varphi_{A_2}(\lambda)$ on the interval $[0, 1]$; (c) figure of function $\varphi_{\Delta}(\lambda)$ on the interval $[0, 1]$; (d) figure of function $\psi_{\Delta}(\lambda)$ on the interval $[0, 1]$.

$$R_s(\psi_{\Delta}) = \begin{vmatrix} 1 & 4 & 8\lambda - 6 & 28\lambda - 34 & 24\lambda - 29 & 0 \\ 0 & 1 & 4 & 8\lambda - 6 & 28\lambda - 34 & 24\lambda - 29 \\ 1 & 0 & h(\lambda) & 0 & 0 & 0 \\ 0 & 1 & 0 & h(\lambda) & 0 & 0 \\ 0 & 0 & 1 & 0 & h(h(\lambda)\lambda) & 0 \\ 0 & 0 & 0 & 1 & 0 & h(\lambda) \end{vmatrix} \quad (51)$$

$$= 256(\lambda - 1)^8.$$

Thus we have a rough summary:

- (i) $\varphi_{A_1}(\lambda)$ is positive (negative) when $\lambda < 2/5$ ($\lambda > 2/5$), and it has a unique zero point $2/5$;
- (ii) $\varphi_{A_2}(\lambda)$ and $\varphi_{\Delta}(\lambda)$ are nonnegative functions defined on interval $(0, 1)$, and they both have the unique zero point $\lambda = 2/5$;
- (iii) $\psi_{\Delta}(\lambda)$ is a negative function defined on interval $(0, 1)$.

Thus, it follows that: (i) $A_1(E_*^{(1)})$ is negative (positive) when $\lambda < 2/5$ ($\lambda > 2/5$); (ii) $A_2(E_*^{(1)})$ and $\Delta_*(E_*^{(1)})$ are always positive when $\lambda \neq 2/5$. In a word, the equilibrium point $E_*^{(1)}$ is a stable or unstable elementary node when $\lambda \neq 2/5$.

On the whole, when $m_2 \neq 2/5a\epsilon$, we have $d_1d_2 \neq 0$, an interior equilibrium point $E_*^{(2)}$ with $A_1 = A_2 = 0$ from the case (C1) is a cusp of codimension 2, and an interior equilibrium point $E_*^{(1)}$ is a stable (unstable) node when $m_2 < 2/5a\epsilon$ ($m_2 > 2/5a\epsilon$). When $m_2 = 2/5a\epsilon$, the unique interior equilibrium point E_* becomes a cusp of codimension at least 3.

Theorem 1. *From the case (C1), when $m_2 \neq 2/5a\epsilon$, an interior equilibrium point $E_*^{(2)}$ with $A_1 = A_2 = 0$ is a cusp of codimension 2 (Bogdanov-Takens bifurcation point) since $d_1d_2 \neq 0$, and an interior equilibrium point $E_*^{(1)}$ is an asymptotic stable (unstable) node when $m_2 < 2/5a\epsilon$ ($m_2 > 2/5a\epsilon$). When $m_2 = 2/5a\epsilon$, the unique interior equilibrium point $E_* = (4a, 5a)$ is a cusp of codimension at least 3, indeed it is a codimension 3 BT singularity (focus or center case), see next subsection.*

Remark 1. When we use the transformations (III): $u = p + a_{02}pq, v = q - a_{20}p^2$, and (IV): $p = w, q = z - c_{11}wz$, the system (29) firstly becomes

$$\begin{aligned} \dot{p} &= q + c_{11}pq + O(|p, q|^3), \\ \dot{q} &= d_{20}p^2 + d_{11}pq + d_{02}q^2 + O(|p, q|^3), \end{aligned} \tag{52}$$

and then becomes

$$\begin{aligned} \dot{w} &= z + O(|w, z|^3), \\ \dot{z} &= f_{20}w^2 + f_{11}wz + f_{02}z^2 + O(|w, z|^3). \end{aligned} \tag{53}$$

Finally, in order to obtain standard form, we construct a transformation (V): $w = x_1 + (1/2)f_{02}x_1^2, z = f_{02}x_1y_1 + y_1$, above system becomes

$$\begin{aligned} \dot{x}_1 &= y_1 + O(|x_1, y_1|^3), \\ \dot{y}_1 &= d_1x_1^2 + d_2x_1y_1 + O(|x_1, y_1|^3). \end{aligned} \tag{54}$$

This also ensures the Theorem 1 and (31).

2.5. Bogdanov-Takens Singularity (Focus or Center) of Codimension 3. Letting $p_x = \Delta_x = 0$ or $p_y = \Delta_y = 0$, we obviously derive thresholds of parameters

$$\begin{aligned} K_1 &= \frac{ar_1(8\alpha e + m_2)}{(r_1 - m_1)(\alpha e - m_2)}, \\ d &= \frac{(8\alpha e + m_2)(\alpha e - m_2)^2}{27\alpha a(r_1 - m_1)e^2}, \end{aligned} \tag{55}$$

and a unique degenerate equilibrium point $E_6 := (x_6, y_6) = ((a(2\alpha e + m_2)/\alpha e - m_2), 18(r_1 - m_1)e^2\alpha a/(8\alpha e + m_2)(\alpha e - m_2))$. In this case, it is quite obvious to see that $A_2(E_6) = 0$, while the trace reduces to

$$A_1(E_6) = \frac{16\alpha^2 e^2 + 6\alpha e m_1 - 14\alpha e m_2 - 6\alpha e r_1 + 3m_1 m_2 - 2m_2^2 - 3m_2 r_1}{3(8\alpha e + m_2)} \tag{56}$$

The combinations in this case with $A_1(E_6) \neq 0$ is denoted as (C4). Furthermore, if $A_1(E_6) = 0$ in the case (C4), thresholds of parameters r_1, K_1, d and a unique nilpotent equilibrium point E_7 are

$$\begin{aligned} r_1 &= \frac{2(\alpha e - m_2)(8\alpha e + m_2) + 3m_1(2\alpha e + m_2)}{3(2\alpha e + m_2)}, \\ K_1 &= \frac{a[2(\alpha e - m_2)(8\alpha e + m_2) + 3m_1(2\alpha e + m_2)]}{2(\alpha e - m_2)^2}, \\ d &= \frac{(2\alpha e + m_2)(\alpha e - m_2)}{18e^2\alpha a}, \end{aligned} \tag{57}$$

$$E_7 := (x_7, y_7) = \left(\frac{a(2\alpha e + m_2)}{\alpha e - m_2}, \frac{12e^2\alpha a}{2\alpha e + m_2} \right).$$

Similarly, we denote this special case as (C5). Note that the conditions (9) (iii) and (9) (iv) all hold in cases (C4) or (C5) since $a_2^2 - 3a_1a_3 = b_2^2 - 3b_1b_3 = 0$.

For the case (C4), we take transformations (I): $x = X + x_6, y = Y + y_6$ and

$$\begin{aligned} (II): X &= \frac{\alpha x_6 u}{a + x_6} + v, \\ Y &= dy_6 u + \frac{3(r_1 - m_1)e}{8\alpha e + m_2} v, \\ \tau &= tA_1. \end{aligned} \tag{58}$$

The system (1) becomes a normal form

$$\dot{u} = u + \Phi(u, v), \tag{59}$$

$$\dot{v} = \Psi(u, v), \tag{60}$$

where $\Phi(u, v), \Psi(u, v) = O(|u, v|^2)$. The implicit function $u = h(v) = h_2v^2 + \dots$ from right hand side of the equation (59) implies $\psi(v) = \Psi(h(v), v) = a_3v^3 + \dots$ with

$$a_3 = \frac{2(r_1 - m_1)(\alpha e - m_2)^3(2\alpha e + m_2)}{27(8\alpha e + m_2)e^2\alpha^2a^2A_1} \neq 0. \tag{61}$$

There is only one zero eigenvalue and a nonzero eigenvalue for the matrix $J(E_6)$, by using the Theorem 7.1 in Zhifen Zhang's book [20], it is easy to see that the equilibrium point E_6 is a stable (unstable) node if $A_1 < 0$ ($A_1 > 0$).

We will provide some explicitly smooth transformations to obtain a normal form with terms up to fourth order and determine the exact type of the equilibrium point E_7 . Firstly, we take a transformation (I): $x = X + x_7, y = Y + y_7$ and translate the equilibrium point E_7 to the origin O . Secondly, we take a linear transformation

$$\begin{aligned} (II): u &= \frac{27(\alpha e - m_2)(2\alpha e + m_2)X}{\alpha(8\alpha e + m_2)^2} - \frac{9(\alpha e - m_2)(2\alpha e + m_2)Y}{\alpha e(8\alpha e + m_2)^2}, \\ v &= \frac{6(\alpha e - m_2)^2X}{\alpha a(8\alpha e + m_2)} + \frac{3(\alpha e - m_2)(2\alpha e + m_2)Y}{e\alpha a(8\alpha e + m_2)}, \end{aligned} \tag{62}$$

and transform matrix $J(E_7)$ to its real Jordan's canonical form, then above system becomes

$$\begin{aligned} \dot{u} &= F_2(u, v) = v + \sum_{i+j=2}^4 a_{ij}u^i v^j + O(|u, v|^5), \\ \dot{v} &= G_2(u, v) = \sum_{i+j=2}^4 b_{ij}u^i v^j + O(|u, v|^5), \end{aligned} \tag{63}$$

where $a_{11} = b_{20} = 0$ and $a_{20}a_{02}b_{11}b_{02} \neq 0$.

Coming to the equation (63), we denote it in obvious notations:

$$\dot{u} = v + \Phi(u, v), \tag{64}$$

$$\dot{v} = \Psi(u, v), \tag{65}$$

where $\Phi(u, v), \Psi(u, v) = O(|u, v|^2)$. Substituting an implicit function $v = h(u) = \alpha_2 u^2 + \alpha_3 u^3 + \dots$ from right hand side of the first equation (64) into the second equation (65), where

$$\begin{aligned}\alpha_2 &= -\frac{2(8\alpha e + m_2)(\alpha e - m_2)}{81e}, \\ \alpha_3 &= \frac{4(\alpha e - m_2)^2(8\alpha e + m_2)}{2187e^2}.\end{aligned}\quad (66)$$

We immediately derive series $\psi(u) = \Psi[u, h(u)] = a_3 u^3 + \dots$, $[\Phi_u(u, v) + \Psi_v(u, v)]|_{v=h(u)} = b_1 u + \dots$ and a discriminant $\mu = b_1^2 + 8a_3$, where

$$\begin{aligned}a_3 &= b_{30} - a_{20}b_{11} = -\frac{4(\alpha e - m_2)^2(8\alpha e + m_2)^2}{6561e^2} < 0, \\ b_1 &= \frac{(\alpha e - m_2)(8\alpha e + 7m_2)(8\alpha e + m_2)}{81e(2\alpha e + m_2)} \neq 0, \\ \mu &= -\frac{(\alpha e - m_2)^2(8\alpha e + m_2)^2(64\alpha^2 e^2 + 16\alpha e m_2 - 17m_2^2)}{6561e^2(2\alpha e + m_2)^2} < 0.\end{aligned}\quad (67)$$

Thus the equilibrium point E_7 is a center or a focus.

Thirdly, we take near identity transformations

$$\begin{aligned}(III): \quad u &= p, v = q - a_{20}p^2 - a_{02}q^2, \\ (IV): \quad p &= w + \frac{1}{2}d_{02}w^2, q = d_{02}wz + z.\end{aligned}\quad (68)$$

To eliminate second order terms in \dot{u} and q^2 term in \dot{q} , thus above system firstly becomes

$$\begin{aligned}\dot{p} &= F_3(p, q) = q + O(|p, q|^3), \\ \dot{q} &= G_3(p, q) = d_{11}pq + d_{02}q^2 + O(|p, q|^3),\end{aligned}\quad (69)$$

and finally becomes

$$\begin{aligned}\dot{w} &= F_4(w, z) = z + \sum_{i+j=3} e_{ij}w^i z^j + O(|w, z|^4), \\ \dot{z} &= G_4(w, z) = f_{11}wz + \sum_{i+j=3} f_{ij}w^i z^j + O(|w, z|^4).\end{aligned}\quad (70)$$

Taking into account $f_{11} = b_{11} + 2a_{20}$ and the Lemma 1, the equilibrium point E_7 is a cusp of codimension at least 3. Obviously, we notice that coefficients $f_{11} \neq 0$, $f_{30} < 0$ and

$$\begin{aligned}5f_{30}(f_{21} + 3e_{30}) - 3f_{11}(f_{40} - e_{30}f_{11}) &= \frac{4(8\alpha e + m_2)^4(56\alpha^2 e^2 - 4\alpha e m_2 - 7m_2^2)(\alpha e - m_2)^3}{14348907(2\alpha e + m_2)^2 e^4} \neq 0, \\ f_{11}^2 + 8f_{30} &= -\frac{(8\alpha e + m_2)^2(64\alpha^2 e^2 + 16\alpha e m_2 - 17m_2^2)(\alpha e - m_2)^2}{6561e^2(2\alpha e + m_2)^2} < 0.\end{aligned}\quad (71)$$

By Lemma 3.1 in paper [21], there must exist a small neighbourhood of the origin O such that the system (70) is locally topologically equivalent to system.

$$\begin{aligned}\dot{x} &= y, \\ \dot{y} &= f_{11}xy + f_{30}x^3 + (f_{21} + 3e_{30})x^2y + (f_{40} - e_{30}f_{11})x^4 \\ &\quad + \left(4e_{40} + f_{31} + \frac{1}{3}e_{21}f_{11} + \frac{1}{6}f_{11}f_{12}\right)x^3y + O(|x, y|^5).\end{aligned}\quad (72)$$

Hence the degenerate equilibrium point E_7 is a codimension 3 Bogdanov-Takens singularity (focus or center). Thus, we have the following theorem:

Theorem 2. *In the cases (C4) and (C5), we have: (i) the equilibrium point E_6 is a stable (unstable) node if $A_1 < 0$ ($A_1 > 0$); (ii) the equilibrium point E_7 is a codimension 3 Bogdanov-Takens singularity (focus or center case).*

2.6. Numerical Simulations and A Brief Summary. This subsection will give numerical simulations for above subsections, which is also a preliminaries of following bifurcations.

2.6.1. The Case (C1)

Example 1. For the case (C1), we set values of some parameters as follow: $r_1 = 0.6$, $\alpha = 0.5$, $a = 1.5$ and $e = 0.6$. For the value $\lambda = (1/2)$, we have: when $\mu = 3 < \mu_\sigma$, the unique equilibrium point E_3 is a stable multiple focus with multiplicity one since the negative first Lyapunov number $\sigma \approx -0.021655 < 0$; when $\mu = \mu_\sigma$, the equilibrium point E_3 is a weak stable focus of order 2; when $\mu = 10 > \mu_\sigma$, the equilibrium point E_3 becomes an unstable multiple focus with multiplicity one; when $\mu = 14 > \mu_1$, the equilibrium point E_3 is a saddle point. A brief inspection in Figure 2 can reveal this phenomenon. Furthermore, it can be noticed that the condition (9) (iii) holds since $a_2^2 - 3a_1a_3 < 0$ when $\mu = 3$.

Figures 3 and 4 include curves of functions $\varphi_{A_2}(\lambda, \mu)$ (red) and $\varphi_\sigma(\lambda, \mu)$ (blue) in the case (C1) corresponding to $\lambda = (1/2)$ and $\lambda = (1/3)$, respectively. Furthermore, it can be noticed that when $\lambda = (1/3)$ with $A_2 > 0$, $\mu_\sigma > \mu_1$ or μ_σ does not exist.

2.6.2. Cases (C2) and (C3). Moreover, as we take $m_2 = (\alpha e/2)(\lambda = (1/2))$, $K_1 = (2(3 + 2\sqrt{2})ar_1/\alpha e)$, $m_1 = r_1 - (3\alpha e/2)$ and $d = ((\sqrt{2} - 1)\alpha/8a)$ to guarantee $A_2(E_4^{(2)}) = 0$

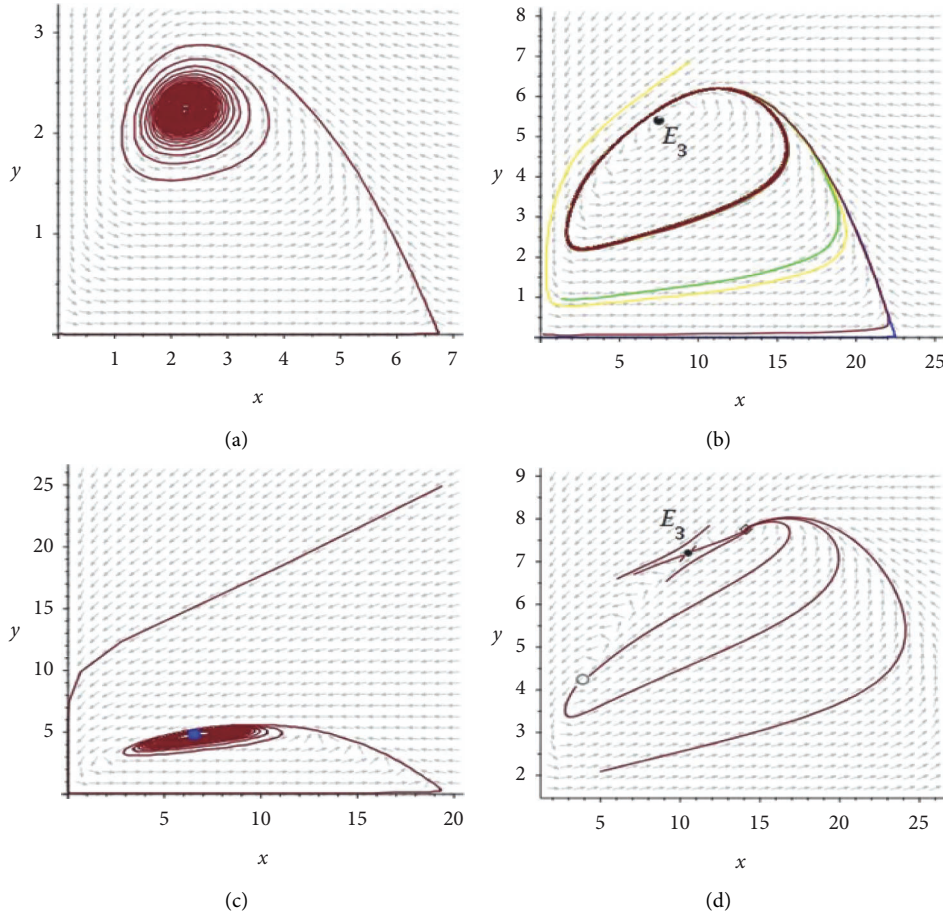


FIGURE 2: Phase diagrams around E_3 in the case (C1) with $(\lambda = (1/2))$: (a) A stable multiple focus with multiplicity one with $\mu = 3$; (b) An unstable multiple focus with multiplicity one with $\mu = 10$; (c) A stable weak focus of order 2 with $\mu = \mu_\sigma$. (d) A saddle point with $\mu = 14$.

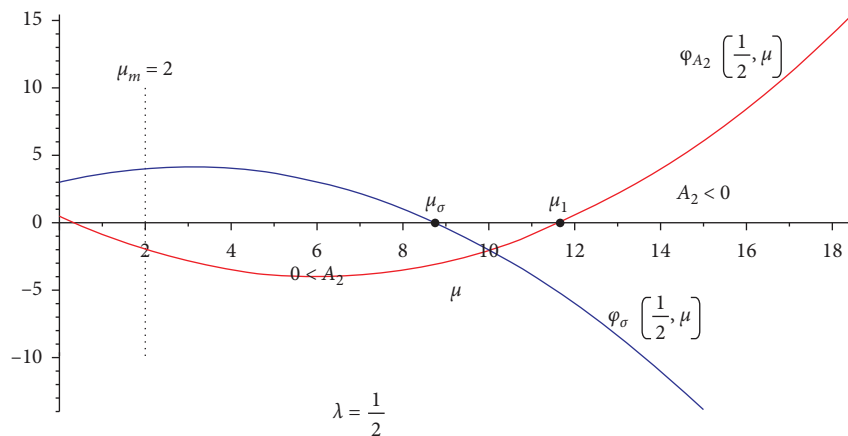


FIGURE 3: Curves of functions $\varphi_{A_2}(\lambda, \mu)$ (in red) and $\varphi_\sigma(\lambda, \mu)$ (in blue) in the case (C1) with $\lambda = (1/2)$.

in the case (C1), then $A_1(E_4^{(2)}) = \Delta_x = \Delta_y = 0$ and our system coexists a degenerate equilibrium point $E_4^{(2)} := (x_4^{(2)}, y_4^{(2)}) = ((3 + 2\sqrt{2})a, 2ae(\sqrt{2} + 2))$ and an unstable node $E_4^{(1)} := (x_4^{(1)}, y_4^{(1)}) = ((1 + 2\sqrt{2})a, 4\sqrt{2}ea)$. We denote this case as (C2).

On the other hand, when we set $m_2 = (ae/3)$ ($\lambda = (1/3)$), $m_1 = r_1 - (4ae/3)$, $K_1 = (3(13 + 3\sqrt{17})ar_1/8ae)$ and $d = ((-5 + 3\sqrt{17})\alpha/72a)$, thus we have $A_1(E_5^{(2)}) = A_2(E_5^{(2)}) = 0$, a nilpotent (or double-zero eigenvalue) $E_5^{(2)} := (x_5^{(2)}, y_5^{(2)}) = (((13 + 3\sqrt{17})a/8), (3ae(7 + \sqrt{17})/$

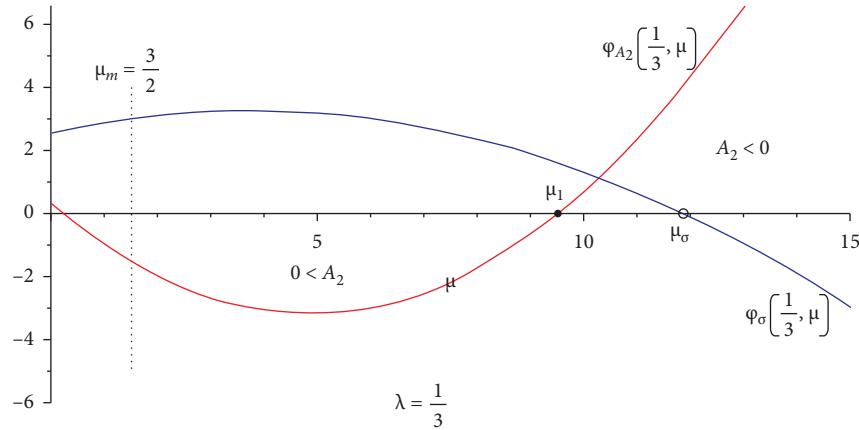


FIGURE 4: Curves of functions $\varphi_{A_2}(\lambda, \mu)$ (in red) and $\varphi_{\sigma}(\lambda, \mu)$ (in blue) in the case (C1) with $(\lambda = (1/3))$.

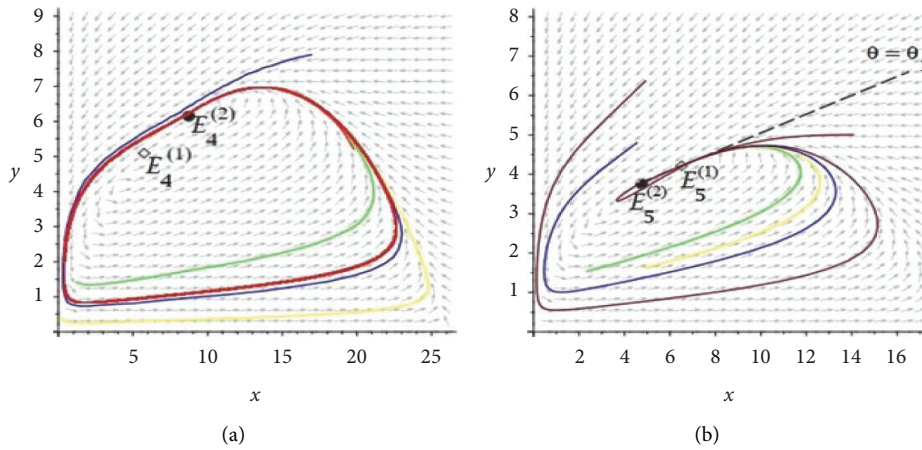


FIGURE 5: (a) A cusp $E_4^{(2)}$ of codimension 2 and an unstable node $E_4^{(1)}$ in the case (C2). (b) A cusp $E_5^{(2)}$ of codimension 2 and a stable node $E_5^{(1)}$ in the case (C3).

8)) and a stable node $E_5^{(1)} := (x_5^{(1)}, y_5^{(1)}) = ((5 + 3\sqrt{17})a/4, (3(\sqrt{17} - 1)ea/2))$. This case is denoted as (C3).

Obeying to Zhifen Zhang’s book [20] once more, for the case (C2) and the system (29), we denote it in analogy with

the equations (64). Then an implicit function from the right hand side of the equation (64) is $v = h(u) = (\alpha(1 - 2\sqrt{2})/16ea^2)u^3 + \dots$. Substituting $v = h(u)$ into the equation (65), we have series

$$\psi(u) = \Psi[u, h(u)] = a_2 u^2 + \dots, a_2 = b_{20} = \frac{(\sqrt{2} - 2)\alpha^2 e}{32a} \neq 0, \tag{73}$$

$$[\Phi_u(u, v) + \Psi_v(u, v)]|_{v=h(u)} = b_1 u + \dots, b_1 = 2a_{20} + b_{11} = \frac{(4 - 5\sqrt{2})\alpha}{8a} \neq 0.$$

Hence the equilibrium point $E_4^{(2)}$ is a degenerate singular point (in the sense of [20]). The point $E_5^{(2)}$ in the case (C3) is also a degenerate singular point since $a_2 = ((-5 + 3\sqrt{17})\alpha^2 e/432a) \neq 0$ and $b_1 = (\alpha(17 - 7\sqrt{17})/36a) \neq 0$.

$E_5^{(2)} \approx (4.756747, 3.754048)$, and a stable node is $E_5^{(1)} \approx (6.513494, 4.216193)$ with characteristic direction $\theta = \theta_1 \approx 0.234711$, which appeals all trajectories in a small neighbourhood of it (see Figure 5(b)).

Example 2. For the cases (C2) and (C3), we take values of parameters from the Example 1. Then a cusp of codimension 2 is $E_4^{(2)} \approx (8.742641, 6.145584)$, and an unstable node is $E_4^{(1)} \approx (5.742641, 5.091169)$, which is surrounded by an closed orbit (see Figure 5(a)); a cusp of codimension 2 is

2.6.3. The Cases (C4) and (C5)

Example 3. For the cases (C4) and (C5), we take some parameters as $\alpha = 0.6, e = 0.9, m_1 = 0.43, m_2 = 0.2$ and $a = 0.125$. A codimension 3 BT singularity equilibrium point

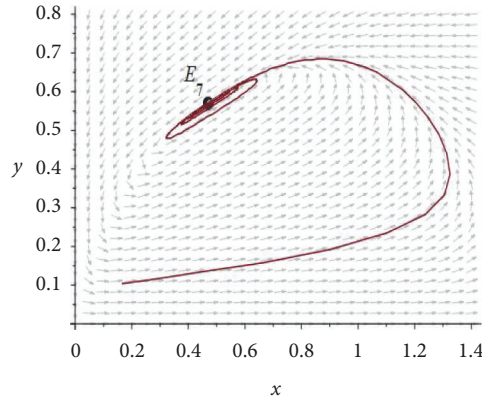


FIGURE 6: A codimension 3 Bogdanov-Takens singularity (focus type) in the case (C5).

is $E_7 \approx (0.470588, 0.569531)$ with $r_1 \approx 1.230417$ (see Figure 6). When $r_1 = 1$, a stable node is $E_6 \approx (0.470588, 0.405580)$ (see Figure 7(a)). While for $r_1 = 1.5$, an unstable node is $E_6 \approx (0.470588, 0.761352)$, and the

Poincare-Bendixson theorem yields that there exists a limit cycle enclosing this equilibrium (see Figure 7(b)).

Finally, at the end of this section, we will conclude stability and type of the equilibrium point E_3 as follows:

$$\begin{aligned}
 \lambda = \frac{2}{5}(\mu_1 = \mu_\sigma, \nexists \mu_\sigma) & \left\{ \begin{array}{l} \text{multiple stable focus with multiplicity one, } \mu < \mu_1, \\ \text{codimension 3 BT singularity (focus or center)} (E_3 \in [E_7]), \mu = \mu_1, \\ \text{saddle point, } \mu > \mu_1; \end{array} \right. \\
 \lambda \in \left(\frac{2}{5}, 1\right)(\mu_1 > \mu_\sigma, \exists \mu_\sigma) & \left\{ \begin{array}{l} \text{multiple stable focus with multiplicity one, } \mu \in (0, \mu_\sigma), \\ \text{weak stable focus of order 2, } \mu = \mu_\sigma, \\ \text{multiple unstable focus with multiplicity one, } \mu \in (\mu_\sigma, \mu_1), \\ \text{cusp of codimension 2} (E_3 \in [E_4^{(2)}]), \mu = \mu_1, \\ \text{saddle point, } \mu > \mu_1; \end{array} \right. \tag{74} \\
 \lambda \in \left(0, \frac{2}{5}\right)(\mu_1 > \mu_\sigma, \nexists \mu_\sigma) & \left\{ \begin{array}{l} \text{multiple stable focus with multiplicity one, } \mu \in (0, \mu_1), \\ \text{cusp of codimension 2} (E_3 \in [E_5^{(2)}]), \mu = \mu_1, \\ \text{saddle point, } \mu > \mu_1. \end{array} \right.
 \end{aligned}$$

In which $[E]$ represents the “equivalence class” of equilibria, which have same properties in stability and type with the representative element E , symbols $\exists \mu_\sigma$ and $\nexists \mu_\sigma$ is the meaning that μ_σ exists and μ_σ does not exist.

3. Local Bifurcations

In this section, more words are included here about the existence of Hopf bifurcation curve in a small neighbourhood of the equilibrium point E_3 in the case (C1), BT bifurcations of codimension 2 in the cases (C2) and (C3), and a

degenerate focus type BT bifurcation of codimension 3 in the case (C5), respectively.

3.1. Hopf Bifurcation Curve Around E_3 . For the case (C1), the system (1) undergoes a nondegenerate Hopf bifurcation around the equilibrium point E_3 as $\sigma \neq 0$. The Hopf bifurcation is supercritical (subcritical) and limit cycles generated by the critical point are stable (unstable) if $\sigma < 0$ ($\sigma > 0$). On occasion, there may exist some parameter values such that $\sigma = 0$ or the system (1) may undergo a degenerate Hopf bifurcation for some values of parameters [17].

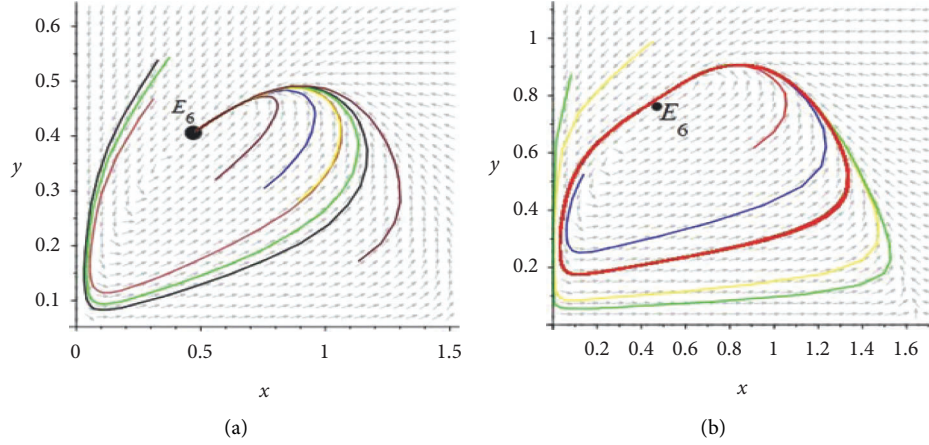


FIGURE 7: Phase diagrams in the case (C4): (a) Stable node E_6 with $r_1 = 1$; (b) Unstable node E_6 with $r_1 = 1.5$.

Conversely, we also study existence of Hopf bifurcation curve in this special case. Choosing m_2 and d as bifurcation parameters and introducing sufficiently small parameter (λ_1, λ_2) . For an unfolding system

$$\begin{aligned} \dot{x} &= x \left[r_1 \left(1 - \frac{x\alpha e}{\mu a r_1} \right) + e(\lambda + 1)\alpha - r_1 - \frac{\alpha y}{a + x} \right], \\ \dot{y} &= y \left[\frac{x\alpha e}{a + x} - \lambda\alpha e - \lambda_1 - \left(-\frac{\lambda\alpha(\lambda\mu - \mu + 1)}{a(\lambda\mu + 1)^2} + \lambda_2 \right) y \right]. \end{aligned} \quad (75)$$

We suppose that the above system has an equilibrium point $E_* = (x_*, y_*)$ when $(\lambda_1, \lambda_2) \neq 0$, where $x_* = x_3 + w$ with $|w| \ll 1$. Calculating $A_1 = 0$ and $A_2 > 0$, we have a solution

$$\begin{aligned} \lambda_1 &= \frac{w\alpha(2a\lambda\mu + a + 2w)}{a(a\lambda\mu + a + w)\mu}, \\ \lambda_2 &= \frac{-\alpha w}{a(a\mu - w)(\lambda\mu + 1)^2((\lambda\mu + 1)a + w)^2} \\ &\left\{ \left((\lambda^3 + \lambda)\mu^2 + (2\lambda^2 + \lambda - 1)\mu + \lambda + 1 \right) (\lambda\mu + 1)a^2 + 2w \left(\begin{aligned} &(\lambda^3 - (1/2)\lambda^2 + (1/2)\lambda)\mu^2 \\ &+ (2\lambda^2 + (1/2)\lambda)\mu + \lambda + 1 \end{aligned} \right) a + w^2(1 + (\lambda - 1)\mu)\lambda \right\}, \end{aligned} \quad (76)$$

with

$$A_2 = \frac{-e^2\alpha^2}{\mu^2 a^2 (a\lambda\mu + a + w)^2} \left\{ (a\lambda\mu + w) \left(\begin{aligned} &(\lambda(\lambda - 1)^2\mu^2 + (2\lambda^2 - 2\lambda - 1)\mu + \lambda)\mu a^3 \\ &+ 5w \left(\frac{1}{5} + \left(\lambda^2 - \left(\frac{6}{5} \right) \lambda + \left(\frac{1}{5} \right) \right) \mu^2 + \left(\left(\frac{6}{5} \right) \lambda - \left(\frac{1}{5} \right) \right) \mu \right) \mu a^2 \\ &+ 8w^2 \left((1/2) + (\lambda - (1/2))\mu \right) a + 4w^3 \end{aligned} \right) \right\}. \quad (77)$$

At this point, the Hopf bifurcation curve of the system (75) is defined by

$$Hp = \{(\lambda_1, \lambda_2) \mid (\lambda_1, \lambda_2) \text{ satisfy (3.2)}\}, \quad (78)$$

and the approximation of Hp is a straight line with slope

$$k = \lim_{w \rightarrow 0} \frac{\lambda_2(w)}{\lambda_1(w)} = \frac{-\mu^2 \lambda^3 - 2\mu \lambda^2 + (-\mu^2 - \mu - 1)\lambda + \mu - 1}{a(\lambda\mu + 1)^2 e(2\lambda\mu + 1)}. \tag{79}$$

In a small neighbourhood of the origin in parameter plane.

Similarly, for the bifurcation parameters m_1 , m_2 and corresponding unfolding system

$$\begin{aligned} \dot{x} &= x \left[r_1 \left(1 - \frac{x\alpha e}{\mu a r_1} \right) + e(\lambda + 1)\alpha - r_1 - \lambda_1 - \frac{\alpha y}{a + x} \right], \\ \dot{y} &= y \left[\frac{x\alpha e}{a + x} - \lambda\alpha e - \lambda_2 + \frac{\lambda\alpha(\lambda\mu - \mu + 1)y}{a(\lambda\mu + 1)^2} \right]. \end{aligned} \tag{80}$$

The Hopf bifurcation curve of the system (80) is defined by

$$\begin{aligned} \lambda_1 &= \frac{\left\{ -w\alpha \left(a^2 \lambda^4 \mu^3 + 3a(a + (2/3)w)\mu^2 \lambda^3 + \mu((\mu^2 + \mu + 3)a^2 - w(\mu - 4)a + w^2)\lambda^2 \right) \right.}{\left. \left(a^2 \lambda^4 \mu^3 + 3a(a + (2/3)w)\mu^2 \lambda^3 + (3(a^2 - (1/3)w(\mu - 4)a + (1/3)w^2))\mu \lambda^2 \right) \mu \lambda^2 \right\} e}{\left\{ \left(a^2 \lambda^4 \mu^3 + 3a(a + (2/3)w)\mu^2 \lambda^3 + (3(a^2 - (1/3)w(\mu - 4)a + (1/3)w^2))\mu \lambda^2 \right) \mu \lambda^2 \right.}, \\ &\quad \left. \left. + (a^2 + 2wa - w^2(\mu - 1))\lambda + wa \right\} a\mu \right\}}, \\ \lambda_2 &= \frac{\left\{ w\alpha \left(a^3 \lambda^5 \mu^4 + (4(a + (3/4)w))a^2 \mu^3 \lambda^4 - ((\mu^2 + \mu - 6)a^2 + w(\mu - 9)a - 3w^2)a\mu^2 \lambda^3 \right) \right.}{\left. - (2((\mu - 2)a^3 + w(\mu - 3/2)(\mu + 3)a^2 + w^2(\mu - 3)a - (1/2)w^3))\mu \lambda^2 \right\} e}{\left\{ (a\lambda\mu + a + w)(a^2 \lambda^4 \mu^3 + 3a(a + (2/3)w)\mu^2 \lambda^3 + (3(a^2 - (1/3)w(\mu - 4)a + (1/3)w^2))\mu \lambda^2 + (a^2 + 2wa - w^2(\mu - 1))\lambda + wa)a\mu \right\}}, \end{aligned} \tag{81}$$

with $A_2 > 0$. Hence the slope of approximation around the origin is

$$k = \lim_{w \rightarrow 0} \frac{\lambda_2(w)}{\lambda_1(w)} = \frac{\lambda \left[1 + (\lambda^3 - \lambda)\mu^3 + (3\lambda^2 - \lambda + 1)\mu^2 + (3\lambda - 1)\mu \right]}{\left[(\lambda^3 + \lambda)\mu^2 + (2\lambda^2 + \lambda - 1)\mu + \lambda + 1 \right] (\lambda\mu + 1)}. \tag{82}$$

From the Example 1 with values of parameters $r_1 = 0.6$, $\alpha = 0.5$, $a = 1.5$ and $e = 0.6$, Figure 8 show the Hopf bifurcation curves with respect to (i) $\lambda = (1/2)$, $\mu = 3$, (ii) $\lambda = (1/2)$, $\mu = 10$, (iii) $\lambda = (1/3)$, $\mu = 3$ and (iv) $\lambda = (1/3)$, $\mu = 10$, respectively. Following subsections will make further efforts to illustrate these curves

3.2. *BT Bifurcations of Codimension 2 Around $E_4^{(2)}$.* In this subsection, we firstly choose m_2 and d as bifurcation parameters, and then investigate BT bifurcation of codimension 2 in the case (C2) by following the techniques and steps in [22, 23] for an unfolding system

$$\begin{aligned} \dot{x} &= x \left[r_1 \left(1 - \frac{x}{K_1} \right) - m_1 - \frac{\alpha y}{a + x} \right], \\ \dot{y} &= y \left[\frac{\alpha e x}{a + x} - (m_2 + \lambda_1) - (d + \lambda_2)y \right], \end{aligned} \tag{83}$$

where parameters λ_1 and λ_2 are sufficiently small. Denoting a provisional parameter vector $\lambda = (\lambda_1, \lambda_2)$ in a small neighbourhood of the origin O , we firstly select a linear transformation (I): $x = X + x_4^{(2)}$, $y = Y + y_4^{(2)}$ to rewrite above system as

$$\begin{aligned} \dot{X} &= F_1(X, Y) = \sum_{i+j=1}^2 a_{ij}(\lambda) X^i Y^j + O(|X, Y|^3), \\ \dot{Y} &= G_1(X, Y) = \sum_{i+j=0}^2 b_{ij}(\lambda) X^i Y^j + O(|X, Y|^3). \end{aligned} \tag{84}$$

Secondly, we should be able to make an affine transformation (II): $u = X$, $v = a_{10}(\lambda)X + a_{01}(\lambda)Y$, then the system (84) is transformed into

$$\begin{aligned} \dot{u} &= F_2(u, v) = v + c_{20}(\lambda)u^2 + c_{11}(\lambda)uv + O(|u, v|^3), \\ \dot{v} &= G_2(u, v) = \sum_{i+j=0}^2 d_{ij}(\lambda)u^i v^j + O(|u, v|^3), \end{aligned} \tag{85}$$

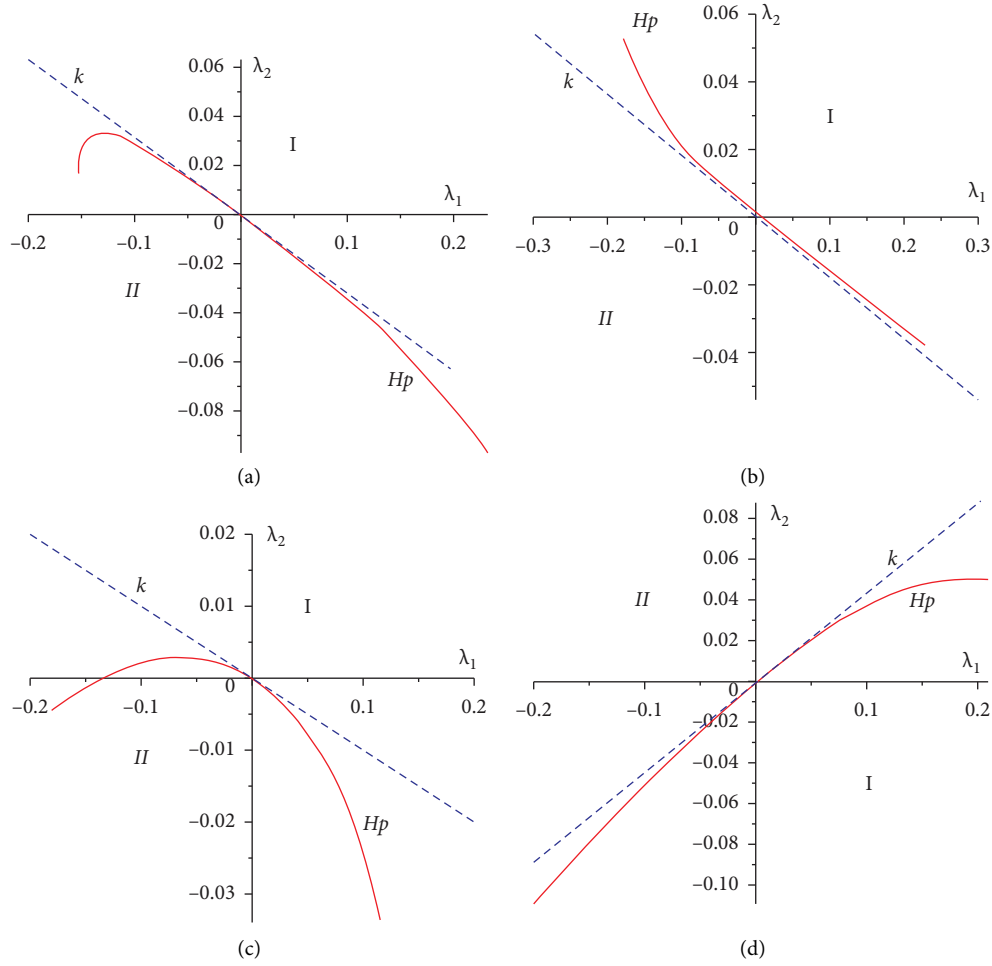


FIGURE 8: (a) Hopf bifurcation curve with $\lambda = (1/2)$ and $\mu = 3$ for the case (C2); (b) Hopf bifurcation curve with $\lambda = (1/2)$ and $\mu = 10$ for the case (C2); (c) Hopf bifurcation curve with $\lambda = (1/3)$ and $\mu = 3$ for the case (C3); (d) Hopf bifurcation curve with $\lambda = (1/3)$ and $\mu = 10$ for the case (C3).

without demur. Thirdly, letting a transformation (III): $p = u - (c_{11}(\lambda) + d_{02}(\lambda)/2)u^2$, $q = c_{20}(\lambda)u^2 - d_{02}(\lambda)uv + v$, we derive a new system

$$\dot{p} = F_3(p, q) = q + O(|p, q|^3), \quad (86)$$

$$\dot{q} = G_3(p, q) = \sum_{i+j=0}^2 f_{ij}(\lambda)p^i q^j + O(|p, q|^3), \quad (87)$$

where $f_{02}(\lambda) = 0$. Finally, in order to eliminate all higher order terms in the equation (86), we mechanically construct a transformation (IV): $w = p$, $z = F_3(p, q)$, then the system (86) is transformed into

$$\begin{aligned} \dot{w} &= F_4(w, z) = z, \\ \dot{z} &= G_4(w, z) = \sum_{i+j=0}^2 h_{ij}(\lambda)w^i z^j + O(|w, z|^3), \end{aligned} \quad (88)$$

where $h_{00}(\lambda) = f_{00}(\lambda)$, $h_{10}(\lambda) = f_{10}(\lambda)$, $h_{01}(\lambda) = f_{01}(\lambda)$ and $h_{02}(\lambda) = 0$. Denoting functions depended on parameters λ_1 and λ_2 :

$$\begin{aligned} d_1(\lambda) &= f_{20}(\lambda), d_1 = d_1(0) = \frac{(4 - 3\sqrt{2})\alpha^2 e^2}{32a}, \\ d_2(\lambda) &= h_{11}(\lambda), d_2 = d_2(0) = \frac{\alpha e(9\sqrt{2} - 14)}{8a}, \end{aligned} \quad (89)$$

$$\xi_1(\lambda) = \frac{f_{00}(\lambda)}{d_1(\lambda)}, \xi_2(\lambda) = \frac{f_{10}(\lambda)}{-d_1(\lambda)}, \eta(\lambda) = \frac{-f_{01}(\lambda)}{\sqrt{-d_1(\lambda)}}$$

$$\Phi(w, \lambda) = f_{00}(\lambda) + f_{10}(\lambda)w + f_{20}(\lambda)w^2 + \dots,$$

and noticing that $d_1, d_2 < 0$, then we take a time transformation (V): $X_1 = -w$, $X_2 = z$, $\tau = -t$ to make it positive and use the Malgrange preparation theorem [24] to obtain a decomposition

$$-\Phi(X_1, \lambda) = (\xi_1(\lambda) + \xi_2(\lambda)X_1 + X_1^2)\Psi(X_1, \lambda), \Psi(0, \lambda) = -d_1(\lambda). \quad (90)$$

Applying a transformation (VI): $Y_1 = X_1$, $Y_2 = (X_2/\sqrt{\Psi(X_1, \lambda)})$, $d\tau = \sqrt{\Psi(X_1, \lambda)}dt$ and a parameter dependent affine transformation (VII): $x = Y_1 + (1/2)\xi_2(\lambda)$, $y = Y_2$, we finally transform above system into the normal form, which still use symbol t as time variable:

$$\begin{aligned} \dot{x} &= y, \\ \dot{y} &= \mu_1(\lambda) + \mu_2(\lambda)y + x^2 + \frac{d_2}{\sqrt{-d_1}}xy + O(|x, y|^3), \end{aligned} \tag{91}$$

where $\mu_1(\lambda) = \xi_1(\lambda) - (1/4)\xi_2(\lambda)^2$ and $\mu_2(\lambda) = \eta(\lambda) - (d_2/2\sqrt{-d_1})\xi_2(\lambda)$. Since the Jacobian

$$\frac{\partial(\mu_1, \mu_2)}{\partial(\lambda_1, \lambda_2)} \Big|_{\lambda=0} = -\frac{128\sqrt{3}\sqrt{2} - 4(1591\sqrt{2} + 2250)a^{(7/2)}}{e\alpha^2} \neq 0, \tag{92}$$

We point out that the above transformation is non-singular, and the results in [25–27] yield that the system (91) is strongly topologically equivalent to system

$$\begin{aligned} \dot{x} &= y, \\ \dot{y} &= \mu_1 + \mu_2 y + x^2 - xy. \end{aligned} \tag{93}$$

In other words, the system (91) will become a standard form

$$\dot{u} = v, \dot{v} = \epsilon_1 + \epsilon_2 v + u^2 - uv + \dots \tag{94}$$

Under a transformation: $x = (-d_1/d_2^2)u$, $y = -(\sqrt{-d_1}/d_2)^3 v$, $t = -(d_2/\sqrt{-d_1})\tau$, where $\epsilon_1 = (d_2/\sqrt{-d_1})^4 \mu_1$ and $\epsilon_2 = -(d_2/\sqrt{-d_1})\mu_2$. Thus, the system (83) will undergo a BT bifurcation with bifurcation parameters μ_1 and μ_2 when parameter λ varies in as small neighbourhood of the origin. Hence, we have following theorem.

Theorem 3 (Bogdanov-Takens bifurcation of codimension 2 around $E_4^{(2)}$). *For the case (C2), in a small neighbourhood of the equilibrium point $E_4^{(2)}$, the system (83) undergoes a*

Bogdanov-Takens bifurcation of codimension 2 when parameter λ varies in a small neighbourhood of the origin when we choose m_2 and d as bifurcation parameters. At the same time, there exist values of parameters such that this system (83) has a limit cycle or a homoclinic loop surround the cusp $E_4^{(2)}$.

Finally, based on the above Theorem 3, the local representations of bifurcation curves up to third-order approximations in a small neighbourhood of the origin with slope $k = (-2 + \sqrt{2}/4ae)$ are presented as follows, including description of saddle-node (SN), Hopf (H) and homoclinic (HL) bifurcation curves [28, 29]. The slope k can be viewed as the limiting case of the slope (79) when $\mu \rightarrow \mu_1$. These bifurcation curves can divide a small neighbourhood of the origin in the parameter plane into several regions, which can exhibit dynamics of the system (83).

(i) The saddle-node bifurcation curve is formulated by

$$\begin{aligned} SN &= \{\lambda \mid \mu_1(\lambda) = 0, \mu_2(\lambda) \neq 0\} \\ &= \left\{ \lambda \mid \lambda_2 = \frac{\sqrt{2} - 2}{4ae} \lambda_1 + O(\lambda_1^2) \right\}, \end{aligned} \tag{95}$$

and

$$\begin{aligned} SN^+ &= \{\lambda \mid \mu_1(\lambda) = 0, \mu_2(\lambda) > 0\}, \\ SN^- &= \{\lambda \mid \mu_1(\lambda) = 0, \mu_2(\lambda) < 0\}. \end{aligned} \tag{96}$$

(ii) The Hopf bifurcation curve is formulated by

$$\begin{aligned} H &= \left\{ \lambda \mid \mu_2(\lambda)^2 - \frac{d_2^2}{d_1} \mu_1(\lambda) = 0, \mu_1(\lambda) < 0 \right\} \\ &= \left\{ \lambda \mid \begin{aligned} &\lambda_1 - \frac{16(81 + 56\sqrt{2})a}{ae} \lambda_1 - \frac{32(274 + 193\sqrt{2})a^2}{\alpha} \lambda_2 \\ &+ \frac{16(713\sqrt{2} + 1000)a}{\alpha^2 e^2} \lambda_1^2 + \frac{128(1067\sqrt{2} + 2269)a^2}{e} \alpha^2 \lambda_1 \lambda_2 \\ &+ \frac{256(3485\sqrt{2} + 4927)a^3}{\alpha^2} \lambda_2^2 - \frac{64(3139 + 2213\sqrt{2})a}{e^3 \alpha^3} \\ &\lambda_1^3 - \frac{128(31753\sqrt{2} + 44932)a^2}{\alpha^3 e^2} \lambda_1^2 \lambda_2 - \frac{256(150706\sqrt{2} + 213155)a^3}{e\alpha^3} \lambda_1 \\ &\lambda_2^2 - \frac{1024(117609\sqrt{2} + 166328)a^4}{\alpha^3} \lambda_2^3 \\ &+ O(|\lambda_1, \lambda_2|^4) = 0, \mu_1(\lambda) < 0 \end{aligned} \right\}. \end{aligned} \tag{97}$$

(iii) The homoclinic bifurcation curve is formulated by

$$\begin{aligned}
 HL = & \left\{ \lambda \mid \mu_2(\lambda)^2 - \frac{25d_2^2}{49d_1^2}\mu_1(\lambda) = 0, \mu_1(\lambda) < 0 \right\} \\
 = & \left\{ \begin{aligned}
 & \lambda \mid -\frac{400(81 + 56\sqrt{2})a}{49\alpha e}\lambda_1 - \frac{800(274 + 193\sqrt{2})a^2}{49\alpha} \\
 & \lambda_2 + \frac{16(17897\sqrt{2} + 25096)a}{49\alpha^2 e^2}\lambda_1^2 + \frac{128(40859\sqrt{2} + 57685)a^2}{49\alpha^2 e}\lambda_1 \\
 & \lambda_2 + \frac{256(93767\sqrt{2} + 132559)a^3}{49\alpha^2}\lambda_2^2 - \frac{64(78787 + 55541\sqrt{2})a}{49e^3\alpha^3} \\
 & \lambda_1^3 - \frac{128(807529\sqrt{2} + 1142740)a^2}{49\alpha^3 e^2}\lambda_1^2 \\
 & \lambda_2 - \frac{256(3995074\sqrt{2} + 5650643)a^3}{49e\alpha^3}\lambda_1 \\
 & \lambda_2^2 - \frac{1024(3358401\sqrt{2} + 4749632)a^4}{49\alpha^3}\lambda_2^3 + O(|\lambda_1, \lambda_2|^4) = 0, \mu_1(\lambda) < 0
 \end{aligned} \right\}. \tag{98}
 \end{aligned}$$

Example 4. The values of parameters will be recalled from the Example 2. Figure 9 gives the saddle-node, Hopf and homoclinic bifurcation curves when the value of parameter λ falls in a small neighbourhood of the origin in the parameter plane. Figures 10–13 depict the dynamics of the system (83) in a small neighbourhood of the origin in the parameter plane when we set values of λ_1 and λ_2 .

- (i) When the value of λ lies on the saddle-node bifurcation curve SN^- , there exist two interior equilibria and one is unstable node.
- (ii) When the value of λ lies on region I (the region below the saddle-node bifurcation curve), there exists a unique unstable node. The Poincaré-Bendixson theorem implies that there is a large limit cycle enclosing this equilibrium point, the detailed numerical simulation results are shown in Figure 10(a) with $(\lambda_1, \lambda_2) \approx (1 \times 10^{-4}, -3.255138 \times 10^{-5})$.
- (iii) When the value of λ lies on another saddle-node bifurcation curve SN^+ , there exists a unique unstable node and a limit cycle.
- (iv) When the value of λ lies on region IV (the region between the saddle-node bifurcation curve SN^+ and the homoclinic curve), there exist an unstable node, a saddle, a stable focus, and the homoclinic loop in case (v) is broken, in which the saddle and the focus are bifurcated from the curve SN^+ , a large limit cycle and enlarged phase diagrams around a stable focus can be seen in Figure 11 with $(\lambda_1, \lambda_2) \approx (1 \times 10^{-4}, -8.131779 \times 10^{-6})$.
- (v) When the value of λ lies on the homoclinic curve, there exist three interior equilibrium points and a homoclinic loop enclosing a stable focus, the detailed numerical simulation results are shown in Figure 12(a) with $(\lambda_1, \lambda_2) \approx (1 \times 10^{-4}, -1.626356 \times 10^{-5})$ and enlarged phase diagrams can be seen in Figure 12(b).
- (vi) When the value of λ crosses the homoclinic curve into region III (the region between the homoclinic curve and the Hopf curve), there exist an unstable node, a saddle and a stable focus, the detailed numerical simulation results are shown in Figure 13 with $(\lambda_1, \lambda_2) \approx (1 \times 10^{-4}, -1.626653 \times 10^{-5})$.
- (vii) When the value of λ lies on the Hopf curve, there exist an unstable node, a saddle, a non-hyperbolic equilibrium point (multiple focus or center) according to Hopf bifurcation and a large limit cycle enclosing these equilibria.
- (viii) When the value of λ crosses the Hopf curve into region II (the region between the Hopf curve and the saddle-node bifurcation curve SN^-), there exist an unstable node, a saddle and an unstable focus, the detailed numerical simulation results are shown in Figure 10(b) with $(\lambda_1, \lambda_2) \approx (1 \times 10^{-4}, -1.627259 \times 10^{-5})$. At the same time, it

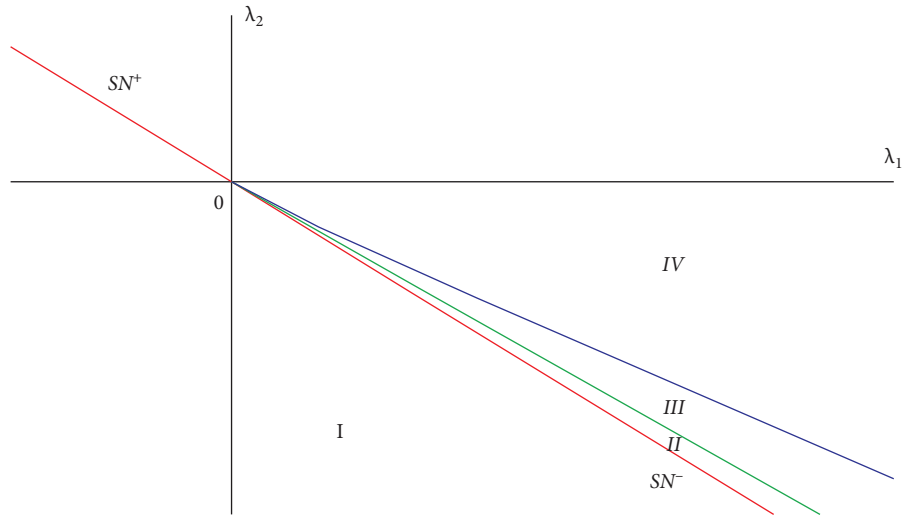


FIGURE 9: Saddle-node (in red), hopf (in green) and homoclinic (in blue) bifurcation curves in case (C2).

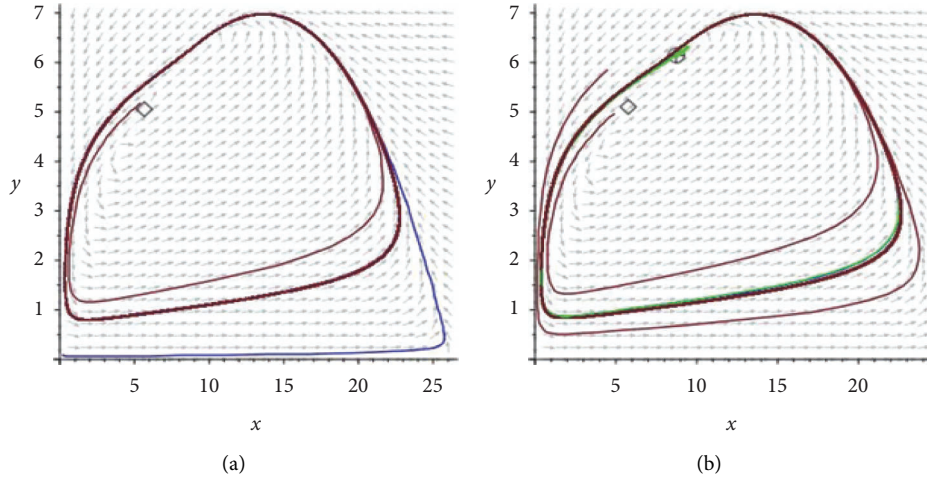


FIGURE 10: Phase diagrams in cases (ii) and (viii).

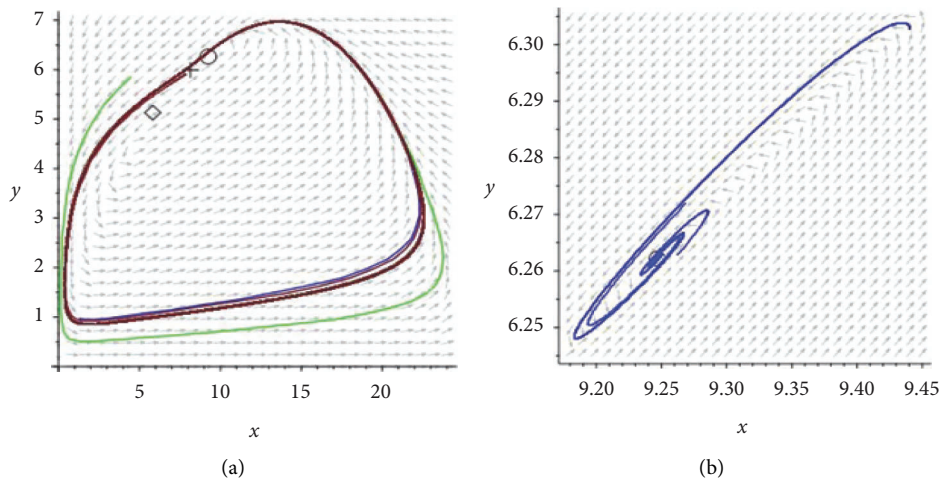


FIGURE 11: Phase diagrams in the case (iv).

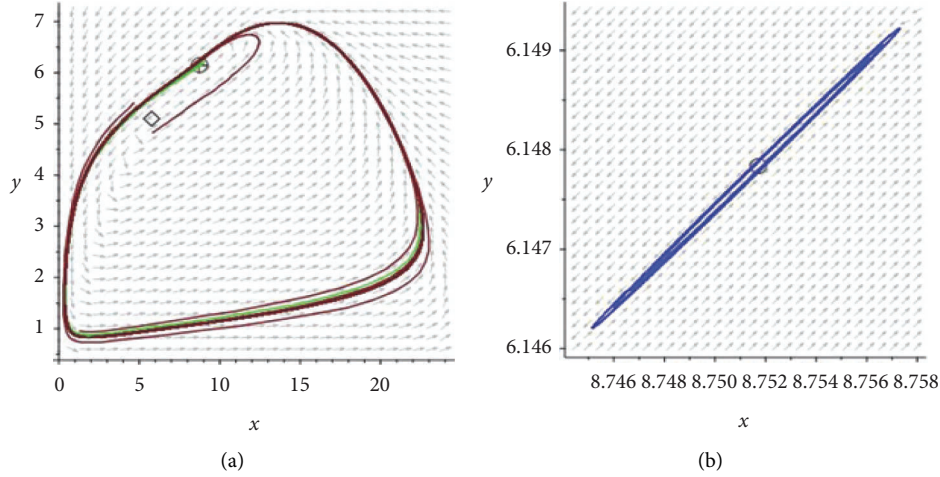


FIGURE 12: Phase diagrams in case (v).

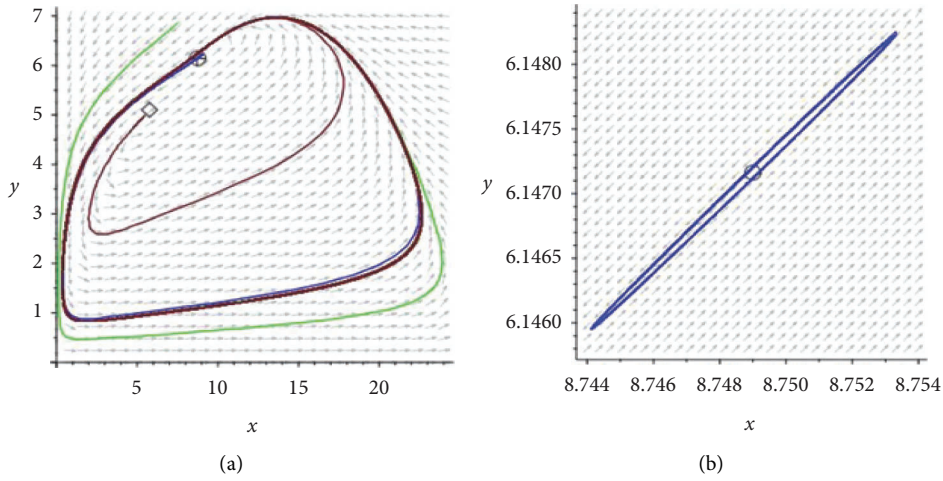


FIGURE 13: Phase diagrams in case (vi).

can be noticed that the stable focus in case (vi) can become unstable.

3.3. BT Bifurcation of Codimension 2 Around $E_5^{(2)}$. In this subsection, we set out to deal with BT bifurcation of codimension 2 around the equilibrium point $E_5^{(2)}$ in the case (C3). Here we choose m_1 and m_2 as bifurcation parameters and rewrite the system (1) as the unfolding form:

$$\begin{aligned} \dot{x} &= x \left[r_1 \left(1 - \frac{x}{K_1} \right) + (m_1 + \lambda_1) - \frac{\alpha y}{a + x} \right], \\ \dot{y} &= y \left[\frac{\alpha e x}{a + x} - (m_2 + \lambda_2) - d y \right], \end{aligned} \quad (99)$$

where λ_1 and λ_2 are sufficiently small parameters and $\lambda = (\lambda_1, \lambda_2)$. Firstly, we take a mere linear transformation (I): $x = X + x_5^{(2)}$, $y = Y + y_5^{(2)}$, the equilibrium point $E_5^{(2)}$ is translated to the origin O :

$$\dot{X} = F_1(X, Y) = \sum_{i+j=0}^2 a_{ij}(\lambda) X^i Y^j + O(|X, Y|^3), \quad (100)$$

$$\dot{Y} = G_1(X, Y) = \sum_{i+j=0}^2 b_{ij}(\lambda) X^i Y^j + O(|X, Y|^3).$$

Secondly, we take a transformation (II): $u = X$, $v = F_1(X, Y)$, then the above system becomes

$$\begin{aligned} \dot{u} &= F_2(u, v) = v, \\ \dot{v} &= G_2(u, v) = \sum_{i+j=0}^2 d_{ij}(\lambda) u^i v^j + O(|u, v|^3). \end{aligned} \quad (101)$$

Thirdly, we take a transformation (III): $p = u + (d_{01}(\lambda)/d_{11}(\lambda))v$, $q = v$ since $d_{11}(0, 0) = ((-85 + 19\sqrt{17})\alpha e / 36a) \neq 0$, then we have following system with $f_{01}(\lambda) = 0$:

$$\begin{aligned} \dot{p} &= F_3(p, q) = q, \\ \dot{q} &= G_3(p, q) = \sum_{i+j=0}^2 f_{ij}(\lambda) p^i q^j + O(|p, q|^3). \end{aligned} \tag{102}$$

Letting (IV): $w = p$, $z = (1 - f_{02}(\lambda)p)q$, $dt = (1 - f_{02}(\lambda)p)d\tau$ and rewrite symbol τ as t , we derive a new system

$$\begin{aligned} \dot{w} &= F_4(w, z) = z, \\ \dot{z} &= G_4(w, z) = \sum_{i+j=0}^2 h_{ij}(\lambda) w^i z^j + O(|w, z|^3). \end{aligned} \tag{103}$$

It can be noticed that $h_{20}(0, 0) = ((33 - 7\sqrt{17})\alpha^2 e^2 / 432a) > 0$ and $h_{11}(0, 0) = d_{11}(0, 0) \neq 0$, so $h_{20}(\lambda) > 0$ and $h_{11}(\lambda) \neq 0$ when λ changes in a small neighbourhood of the origin, which depends smoothly on λ . Finally, we construct a time transformation (V): $m = (h_{11}(\lambda)^2 / h_{20}(\lambda))w$, $n = (h_{11}(\lambda)^3 / h_{20}(\lambda)^2)z$, $dt = (h_{11}(\lambda) / h_{20}(\lambda))d\tau$ and rewrite symbol τ as t , then the above system (103) becomes

$$\begin{aligned} \dot{m} &= F_5(m, n) = n, \\ \dot{n} &= G_5(m, n) \\ &= \mu_1(\lambda) + \mu_2(\lambda)m + m^2 + mn + O(|m, n|^3), \end{aligned} \tag{104}$$

where

$$\begin{aligned} \mu_1 &= \mu_1(\lambda) \\ &= \frac{578(1 - \sqrt{17})}{\alpha e} \lambda_1 + \frac{867(9 - \sqrt{17})}{\alpha e} \lambda_2 + O(|\lambda_1, \lambda_2|^2), \\ \mu_2 &= \mu_2(\lambda) \\ &= \frac{2(-51 + 11\sqrt{17})}{\alpha e} \lambda_1 + \frac{6(9\sqrt{17} - 85)}{\alpha e} \lambda_2 + O(|\lambda_1, \lambda_2|^2). \end{aligned} \tag{105}$$

Therefore, owing to the Jacobian of μ_1 and μ_2

$$\frac{\partial(\mu_1, \mu_2)}{\partial(\lambda_1, \lambda_2)} \Big|_{\lambda=0} = \frac{3468(85 + 19\sqrt{17})}{\alpha^2 e^2} \neq 0, \tag{106}$$

or

$$-\frac{1}{(\partial\mu_1/\partial\lambda_2)} \cdot \frac{\partial(\mu_1, \mu_2)}{\partial(\lambda_1, \lambda_2)} \Big|_{\lambda=0} < 0. \tag{107}$$

The system (99) is a generic family unfolding at the codimension 2 cusp $E_5^{(2)}$, and we have following local representations of the bifurcation curves up to second-order approximations with slope $k = ((1 + \sqrt{17})/12)$ for the system (104) [30]. Thus, it can be noticed that this slope k can be viewed as the limiting case of the slope (82) when $\mu \rightarrow \mu_1$.

(i) The saddle-node bifurcation curve is formulated by

$$\begin{aligned} SN &= \left\{ \lambda \mid \mu_1 = \frac{1}{4}\mu_2^2 \right\} \\ &= \left\{ \begin{aligned} &\lambda \left| \frac{578(1 - \sqrt{17})}{\alpha e} \lambda_1 + \frac{867(9 - \sqrt{17})}{\alpha e} \lambda_2 + \frac{17(9775 - 63\sqrt{17})}{2\alpha^2 e^2} \lambda_1^2 \right. \\ &\left. + \frac{255(1003 - 499\sqrt{17})}{\alpha^2 e^2} \lambda_1 \lambda_2 + \frac{306(3111 - 623\sqrt{17})}{\alpha^2 e^2} \lambda_2^2 + O(|\lambda_1, \lambda_2|^3) = 0 \right. \end{aligned} \right\}. \end{aligned} \tag{108}$$

(ii) The Hopf bifurcation curve is formulated by

$$\begin{aligned} H &= \{ \lambda \mid \mu_1 = 0, \mu_2 < 0 \} \\ &= \left\{ \begin{aligned} &\lambda \left| \frac{578(1 - \sqrt{17})}{\alpha e} \lambda_1 + \frac{867(9 - \sqrt{17})}{\alpha e} \lambda_2 + \frac{51(3441 - 65\sqrt{17})}{2\alpha^2 e^2} \lambda_1^2 \right. \\ &\left. + \frac{51(5723 - 2659\sqrt{17})}{\alpha^2 e^2} \lambda_1 \lambda_2 + \frac{1224(841 - 167\sqrt{17})}{\alpha^2 e^2} \lambda_2^2 \right. \\ &\left. + O(|\lambda_1, \lambda_2|^3) = 0 \right. \end{aligned} \right\}. \end{aligned} \tag{109}$$

(iii) The homoclinic bifurcation curve is formulated by

$$HL = \left\{ \lambda \mid \mu_1 = -\frac{6}{25}\mu_2^2, \mu_2 < 0 \right\}$$

$$= \left\{ \begin{aligned} & \lambda \left[\frac{578(1 - \sqrt{17})}{\alpha e} \lambda_1 + \frac{867(9 - \sqrt{17})}{\alpha e} \lambda_2 + \frac{51(90409 - 2681\sqrt{17})}{50\alpha^2 e^2} \lambda_1^2 \right. \\ & \left. + \frac{51(160067 - 70411\sqrt{17})}{25\alpha^2 e^2} \lambda_1 \lambda_2 + \frac{1224(22543 - 4445\sqrt{17})}{25\alpha^2 e^2} \lambda_2^2 + O(|\lambda_1, \lambda_2|^3) \right] = 0 \end{aligned} \right\}. \tag{110}$$

Theorem 4 (Bogdanov-Takens bifurcation of codimension 2 around $E_5^{(2)}$). For the case (C3), in a small neighbourhood of the equilibrium point $E_5^{(2)}$, there exist values of parameters such that the system (99) undergoes an attracting Bogdanov-Takens bifurcation of codimension 2 when parameter λ varies in a small neighbourhood of the origin with bifurcation parameters m_1 and m_2 . And this system is a generic family unfolding at the cusp $E_5^{(2)}$ of codimension 2.

Example 5. Here we extract values of parameters in the Subsection 3.2 and the Example 3. Figure 14 presents the saddle-node, Hopf and homoclinic bifurcation curves when the value of parameter λ falls in a small neighbourhood of the origin in the parameter plane, which can divide a small neighbourhood of the origin in the parameter plane into several regions and exhibit different dynamical behavior of the system (99).

- (i) When the value of λ crosses the λ_1 axis into region I (the region between the saddle-node bifurcation curve SN_2 and the homoclinic bifurcation curve), there exist an unstable focus, a saddle and a stable node, in which the focus and saddle are bifurcated from the curve SN_2 .
- (ii) When the value of λ lies on the homoclinic bifurcation curve, there exist a saddle, a stable node and a homoclinic loop enclosing an unstable focus.
- (iii) When the value of λ crosses the homoclinic bifurcation curve into region II (the region between the homoclinic bifurcation curve and the Hopf bifurcation curve), there exist an unstable focus, a saddle and a stable node.
- (iv) When the value of λ lies on the Hopf bifurcation curve, there exist three interior equilibria including a saddle and a stable node.
- (v) When the value of λ crosses the Hopf bifurcation curve into region III (the region between the Hopf bifurcation curve and the saddle-node bifurcation curve SN_1), there exist a stable focus, a saddle and a stable node. Furthermore, it shall be noticed that the unstable focus in case (iii) becomes stable, which can ensure potential Hopf bifurcation.
- (vi) When the value of λ lies on the saddle-node bifurcation curve SN_1 , there exist two interior equilibria including a stable node.
- (vii) When the value of λ crosses the saddle-node bifurcation curve into region IV (the region above

the saddle-node bifurcation curve), there exists a unique stable node.

- (viii) When the value of λ lies on the saddle-node bifurcation curve SN_2 , the unique equilibrium point is a stable node.

3.4. Degenerate Focus Type BT Bifurcation of Codimension 3.

We should always keep the case (C5) in mind and choose r_1, K_1 and d as bifurcation parameters and use the method in [14]. Thus we introduce sufficiently small variables $\alpha_1, \alpha_2, \alpha_3$, a parameter vector $\mathcal{A} = (\alpha_1, \alpha_2, \alpha_3)$, the origin $O = (0, 0, 0)$ in parameter space and an unfolding form system

$$\dot{x} = x(r_1 + \alpha_1) \left(1 - \frac{x}{K_1 + \alpha_2} \right) - \frac{\alpha x y}{a + x} - m_1 x,$$

$$\dot{y} = \frac{\alpha e x y}{a + x} - m_2 y - (d + \alpha_3) y^2. \tag{111}$$

Of the system (1) since the Theorem 2 (ii). As indicated in Subsection 2.5 for the system (111), by using the coordinate transformations (I), (II), (III) and (IV), actual calculations can yield a new system

$$\dot{w} = F_4(w, z) = \sum_{i+j=0}^3 e_{ij}(\mathcal{A}) w^i z^j + O(|w, z|^4), \tag{112}$$

$$\dot{z} = G_4(w, z) = \sum_{i+j=0}^3 f_{ij}(\mathcal{A}) w^i z^j + O(|w, z|^4). \tag{113}$$

Here we omit complicated, but consider inconsequential expressions of smooth functions $e_{ij}(\mathcal{A})$ and $f_{ij}(\mathcal{A})$ for the sake of convenience, while $e_{ij}(0) = e_{ij}, f_{ij}(0) = f_{ij}$, for instance, $e_{00}(0) = e_{10}(0) = e_{20}(0) = e_{11}(0) = e_{02}(0) = 0$ and $f_{00}(0) = f_{10}(0) = f_{01}(0) = f_{20}(0) = f_{02}(0) = 0$.

Secondly, in order to eliminate third-order terms in right hand side of equation (112) when $\mathcal{A} = 0$, we construct a transformation

$$(V): \begin{aligned} w &= x_1 + e_{03} x_1 y_1^2, \\ z &= -e_{12} x_1 y_1^2 - e_{21} x_1^2 y_1 - e_{30} x_1^3 + y_1. \end{aligned} \tag{114}$$

Above system becomes

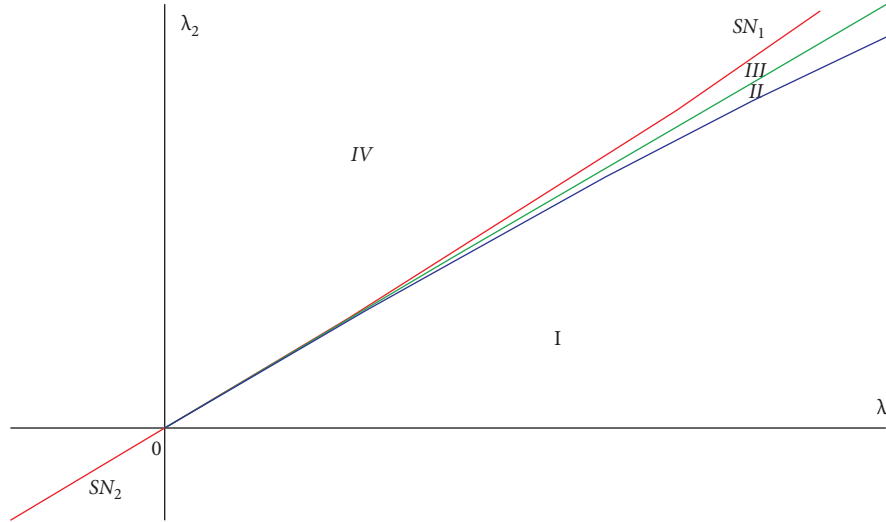


FIGURE 14: Saddle-node (in red), hopf (in green) and homoclinic (in blue) bifurcation curves in the case (C3).

$$\begin{aligned} \dot{x}_1 &= F_5(x_1, y_1) = y_1 + \sum_{i+j=0}^3 g_{ij}(\mathcal{A})x_1^i y_1^j + O(|x_1, y_1|^4), \\ \dot{y}_1 &= G_5(x_1, y_1) = \sum_{i+j=0}^3 h_{ij}(\mathcal{A})x_1^i y_1^j + O(|x_1, y_1|^4). \end{aligned} \tag{115}$$

Similarly, coefficients $g_{ij}(\mathcal{A})$, $h_{ij}(\mathcal{A})$ are all omitted for space and can be deduced by coefficients $e_{ij}(\mathcal{A})$ and $f_{ij}(\mathcal{A})$. Moreover, it shall be noticed that $g_{ij}(0) = 0 (i + j \leq 3)$. Finally, the transformation (VI): $x_2 = x_1, y_2 = F_5(x_1, y_1)$ can translate the above system into the following system

$$\begin{aligned} \dot{x}_2 &= F_6(x_2, y_2) = y_2, \\ \dot{y}_2 &= G_6(x_2, y_2) \\ &= \sum_{i+j=0}^3 k_{ij}(\mathcal{A})x_2^i y_2^j + O(|x_2, y_2|^4), \end{aligned} \tag{116}$$

where coefficients $k_{ij}(\mathcal{A})$ can be expressed by $g_{ij}(\mathcal{A})$ and $h_{ij}(\mathcal{A})$ recursively, and we also omit them here since they are much too tedious.

In addition, it shall be noticed that

$$\begin{aligned} k_{30}(0) &= \frac{4(ae - m_2)^2 (8ae + m_2)^2}{6561e^2} < 0, \\ k_{21}(0) &= \frac{(ae - m_2)(8ae + m_2)^2 (64a^2e^2 - 20aem_2 - 35m_2^2)}{8748(2ae + m_2)^2 e^2} < 0. \end{aligned} \tag{117}$$

Combining the paper [14, 31] and making a time transformation $\tau = -((k_{30}(\mathcal{A})/(k_{21}(\mathcal{A})))t$ in a small neighbourhood of $\mathcal{A} = 0$ (we still use symbol t), the new version of the system (116)

$$\begin{aligned} \dot{u} &= \frac{\sigma(\mathcal{A})}{\nu(\mathcal{A})} v, \\ \dot{v} &= \frac{k_{30}(\mathcal{A})}{\sigma(\mathcal{A})} [\lambda_1(\mathcal{A}) + \lambda_2(\mathcal{A})\nu(\mathcal{A})u - \nu(\mathcal{A})^3 u^3] \\ &\quad + k_{21}(\mathcal{A}) [\lambda_3(\mathcal{A}) + A(\mathcal{A})\nu(\mathcal{A})u + \nu(\mathcal{A})^2 u^2] + \nu^2 Q_1(u, \nu, \mathcal{A}) + O(|u, \nu|^4), \end{aligned} \tag{118}$$

can be rewritten as

$$\begin{aligned} \dot{u} &= v, \\ \dot{v} &= \mu_1(\mathcal{A}) + \mu_2(\mathcal{A})u - u^3 + \nu [\mu_3(\mathcal{A}) + A_1(\mathcal{A})u + u^2] + \nu^2 Q_2(u, \nu, \mathcal{A}) + O(|u, \nu|^4), \end{aligned} \tag{119}$$

where coefficients are

$$\begin{aligned} \lambda_1(\mathcal{A}) &= \frac{k_{00}(\mathcal{A})}{k_{30}(\mathcal{A})} + \frac{k_{10}(\mathcal{A})k_{20}(\mathcal{A})}{3k_{30}(\mathcal{A})^2} - \frac{k_{20}(\mathcal{A})^3}{9k_{30}(\mathcal{A})^3} + \frac{k_{20}(\mathcal{A})^3}{27k_{30}(\mathcal{A})^3}, \\ \lambda_2(\mathcal{A}) &= \frac{k_{10}(\mathcal{A})}{k_{30}(\mathcal{A})} + \frac{k_{20}(\mathcal{A})^2}{3k_{30}(\mathcal{A})^2}, \\ \lambda_3(\mathcal{A}) &= \frac{k_{01}(\mathcal{A})}{k_{21}(\mathcal{A})} - \frac{k_{11}(\mathcal{A})k_{20}(\mathcal{A})}{3k_{21}(\mathcal{A})k_{30}(\mathcal{A})} + \frac{k_{21}(\mathcal{A})k_{20}(\mathcal{A})^2}{9k_{21}(\mathcal{A})k_{30}(\mathcal{A})^2}, \\ A(\mathcal{A}) &= \frac{k_{11}(\mathcal{A})}{k_{21}(\mathcal{A})} + \frac{2k_{20}(\mathcal{A})}{3k_{30}(\mathcal{A})}, \\ \nu(\mathcal{A}) &= \sqrt{\frac{k_{30}(\mathcal{A})}{k_{21}(\mathcal{A})^2}}, \\ \sigma(\mathcal{A}) &= -\frac{k_{30}(\mathcal{A})}{k_{21}(\mathcal{A})} \nu(\mathcal{A}), \\ Q_1(u, v, \mathcal{A}) &= \sigma(\mathcal{A}) \left[k_{02}(\mathcal{A}) + \frac{k_{12}(\mathcal{A})k_{20}(\mathcal{A})^2}{9k_{30}(\mathcal{A})^2} + \sigma(\mathcal{A})k_{03}(\mathcal{A})\nu + \nu(\mathcal{A})k_{12}(\mathcal{A})u \right], \\ A_1(\mathcal{A}) &= \frac{k_{21}(\mathcal{A})\sqrt{-k_{30}(\mathcal{A})}}{k_{30}(\mathcal{A})} A(\mathcal{A}), \\ Q_2(u, v, \mathcal{A}) &= -\frac{k_{21}(\mathcal{A})}{k_{30}(\mathcal{A})} Q_1(u, v, \mathcal{A}), \end{aligned} \tag{120}$$

and a transformation is

$$\begin{aligned} \mu_1(\mathcal{A}) &= \frac{k_{21}(\mathcal{A})^3}{k_{30}(\mathcal{A})\sqrt{-k_{30}(\mathcal{A})}} \lambda_1(\mathcal{A}), \\ \mu_2(\mathcal{A}) &= -\frac{k_{21}(\mathcal{A})^2}{k_{30}(\mathcal{A})} \lambda_2(\mathcal{A}), \\ \mu_3(\mathcal{A}) &= -\frac{k_{21}(\mathcal{A})^2}{k_{30}(\mathcal{A})} \lambda_3(\mathcal{A}). \end{aligned} \tag{121}$$

With some necessary calculations, we can derive

$$\begin{aligned} A_1(0) &= -\frac{8\alpha e + 7m_2}{2(2\alpha e + m_2)} < 0, \\ \frac{\partial(\mu_1, \mu_2, \mu_3)}{\partial(\alpha_1, \alpha_2, \alpha_3)} \Big|_{\mathcal{A}=0} &= \frac{-9e(64\alpha^2 e^2 - 20\alpha e m_2 - 35m_2^2)^6}{131072(16\alpha^2 e^2 + 6\alpha e m_1 - 14\alpha e m_2 + 3m_1 m_2 - 2m_2^2)(2\alpha e + m_2)^{12}} \neq 0. \end{aligned} \tag{122}$$

That is to say, the transformation (121) is a homeomorphism and independent in a small neighbourhood of the origin. By the results of [14, 31–33], the above system (119) is

a generic three parameters family or standard family of BT singularity of codimension 3 (focus case). Hence, the system (1) in the case (C5) undergoes a degenerate focus type BT

bifurcation of codimension 3 with the value of bifurcation parameters r_1, K_1 and d falling in a small neighbourhood of E_7 .

Theorem 5 (Degenerate focus type Bogdanov-Takens bifurcation of codimension 3). *For the case (C5), if the variable \mathcal{A} falls in a small neighbourhood of the origin, then the system (111) undergoes a degenerate focus type BT bifurcation of codimension 3 in a small neighbourhood of E_7 . In a sufficiently small neighbourhood of (r_1, K_1, d) of the bifurcation parameter space, there is a Hopf bifurcation surface, two homoclinic bifurcation surfaces, two saddle-node loop bifurcation surfaces, a multiple limit cycle bifurcation surface, and two saddle-node bifurcation surfaces for the system (111). When parameters (r_1, K_1, d) cross above surfaces, the system (111) undergoes above bifurcations, respectively.*

Example 6. We take out values of parameters from the Example 3, the system (111) undergoes a degenerate focus type Bogdanov-Takens bifurcation of codimension 3 in a small neighbourhood of E_7 when the variable vector $\mathcal{A} = (\alpha_1, \alpha_2, \alpha_3)$ varies in a small neighbourhood of the origin O .

4. Summary

In summary, the main object of writing this paper is to consider Hopf and BT bifurcations of codimension 2 and 3 in the Bazykin’s predator-prey system. The system in our paper has complicated and rich dynamical behaviors. The particular cases (C1)–(C5) based on polynomial equations and Jacobian matrix at point E_* are analytical obtained and investigated in detail. In the case (C1), for the equilibrium point E_3 , with the normal form and the Lyapunov number at hand, we analyze the stability, Hopf bifurcation with standard bifurcation theory and existence of Hopf bifurcation curve with bifurcation parameters m_1 and d . In the cases (C2) and (C3), the equilibria $E_4^{(2)}$ and $E_5^{(2)}$ are both cusp of codimension 2, and we analytically give formulae of saddle-node, Hopf and homoclinic bifurcation curves, respectively. These bifurcation curves can divide a small neighbourhood of the origin in the parameter plane into several regions, which can exhibit dynamical behaviors of corresponding unfolding system, respectively. In the case (C5), the nilpotent equilibrium point E_7 is a codimension 3 BT singularity (focus or center), which can exhibit a degenerate focus type BT bifurcation of codimension 3 in a small neighbourhood. For the system (1) or a general ODEs system, some open problems are:

- (i) Whether the BT bifurcations in Subsection 3.2 and Subsection 3.3 are limiting cases of the Hopf bifurcations in Subsection 3.1 when $\mu \rightarrow \mu_1$?
- (ii) The existence and uniqueness of a codimension N cusp, and the corresponding bifurcation;
- (iii) Whether a codimension $N + 1$ cusp (bifurcation) is the threshold or limiting case of some codimension N cusps (bifurcations) or not?

- (iv) The classification work of a codimension N cusp, for instance, topologically equivalent systems, diffeomorphic systems, limit cycles or homoclinic loops;
- (v) The existence of invariant quantities under some nonsingular transformations, for instance, the Lyapunov quantities, the symbolled “index” $\text{sgn}(d_1 d_2) = \pm 1$ or 0 within codimension 2 cusps. Correspondingly, a codimension 2 and 3 cusps respectively signifies $\text{sgn}(d_1 d_2) = \pm 1$ and $\text{sgn}(d_1 d_2) = 0$.

Besides to the Theorem 3, Theorem 4 and Theorem 5, in a sense, we point out that the maximum number of limit cycles in our system is an important research content, particularly the versal unfolding of a focus type BT singularity of codimension 3. These are reflected in the open problems in [34] or the Hilbert’s 16th problem. Up to now, the Poincare-Bendixson’s existence theorem, the Zhifen Zhang’s uniqueness theorem and the Wintner-Perko termination principle to determine at most two limit cycles surrounding a singular point in [35, 36] are functional tools. Aparting from these theorems, the Theorem 5.4 (ii) in [37] established a result that there exists a unique stable limit cycle in the first quadrant if required condition holds; the Theorem 4, Corollary 1 and Corollary 2 in [38] proved that the system has at least one stable limit cycle and one unstable limit cycle.

Based on above open problem (iv), the paper [10] mainly gave occurrence of Bogdanov-Takens bifurcations and modified the approximate calculation of limit cycles via a perturbation procedure and canonical transformation in view of supercritical Hopf bifurcation. It further illustrate the BT singularity (focus or center) E_7 of codimension 3, which also shows its uniqueness and nonexistence of codimension $N \geq 4$ cusps. Finally, it is our expectancy that the qualitative analysis of stability and bifurcations can be suitable to more predator-prey systems to reveal these phenomena, which are much more complex and have richer dynamical behaviors, even physical mechanical systems and epidemic models, etc.

In the follow-up research works, we will first deepen theoretical research of bifurcation dynamics by learning from relevant results in these papers [39–41], and then further explore the dynamic behavior of patch pattern in ecosystem in the help of these papers [42–44], finally put mathematical models in specific ecological and environmental problems to study their ecological significance by means of these papers [45–47]. In a word, all these results are expected to be useful in studying dynamic behavior of the ecosystem.

Appendix: The Second Focal Quantity

After reducing a_{30} , all coefficients in the second focal quantity $g_5 = 1/144\beta^4 \sum_{k=0}^3 \beta^k g_k^{(5)}$ are

$$g_3^{(5)} = 9(a_{32} + 5a_{50} + 5b_{05} + b_{23} + b_{41} + a_{14}),$$

$$g_2^{(5)} = 3 \begin{bmatrix} (9a_{31} + 22b_{04} + 4b_{22} - 6b_{40} + 7a_{13})a_{20} + (-22a_{40} - 9b_{13} - 7b_{31} + 6a_{04} - 4a_{22})b_{02} \\ + (5a_{13} + 3a_{31} + 20b_{04} + 2b_{22})a_{02} + (-5a_{40} - 2b_{31} + 3a_{04} + a_{22})a_{11} \\ + (b_{12} + 3a_{03} + 3b_{30} + a_{21})a_{12} + (-3b_{12} + 9a_{03} + 9b_{30} - 3a_{21})b_{03} \\ + (5b_{04} - b_{22} - 3b_{40} + 2a_{13})b_{11} + (-20a_{40} - 3b_{13} - 5b_{31} - 2a_{22})b_{20} \\ - 2b_{21}(b_{12} + a_{21}) \end{bmatrix},$$

$$g_1^{(5)} = (15b_{03} + 14b_{21} - 13a_{12})b_{02}^2 + (24a_{03} - 30b_{12} + 24b_{30} - 30a_{21})a_{20}$$

$$+ (48a_{03} - 24b_{12} + 18b_{30} - 18a_{21})a_{02} + (-12b_{03} + 5b_{21} - 7a_{12})a_{11}$$

$$+ (3a_{03} + 12b_{12} + 12b_{30} + 3a_{21})b_{11} + 10b_{20}\left(b_{21} - 2a_{12} - \left(\frac{21}{5}\right)b_{03}\right)b_{02}$$

$$+ (-15b_{03} - 18b_{21} + 9a_{12})a_{20}^2 + (42b_{03} - 6b_{21} + 24a_{12})a_{02}$$

$$+ (21a_{03} + 12b_{30} + 9a_{21})a_{11} + (12b_{03} - 3b_{21} + 9a_{12})b_{11}$$

$$- \left(12\left(b_{12} - \left(\frac{5}{2}\right)b_{30} + (3/2)a_{21}\right)b_{20}\right)a_{20} + (45b_{03} + 15a_{12})a_{02}^2$$

$$+ ((24a_{03} + 3b_{12} + 9b_{30} + 6a_{21})a_{11} + (12b_{03} - 3b_{21} + 9a_{12})b_{11} - 6b_{20}(b_{12} + a_{21}))a_{02}$$

$$+ (-3b_{03} - b_{21} + 2a_{12})a_{11}^2 + \left((6a_{03} + 6b_{30})b_{11} + 5b_{20}\left(b_{21} - \left(\frac{7}{5}\right)a_{12} - \left(\frac{12}{5}\right)b_{03}\right)\right)a_{11}$$

$$+ (3b_{03} + 3b_{21})b_{11}^2 + \left(9\left(b_{12} + \left(\frac{5}{3}\right)b_{30} + (2/3)a_{21}\right)\right)b_{20}b_{11} - 15b_{20}^2(a_{12} + 3b_{03}),$$

$$g_0^{(5)} = (10a_{02} - 5b_{11} + 18a_{20})b_{02}^3 + ((-28b_{20} - 21a_{11})a_{02} + (-10a_{20} + 4b_{11})a_{11} + 20a_{20}b_{20})b_{02}^2$$

$$+ (30a_{02}^3 + (18a_{20} + 3b_{11})a_{02}^2 + (-9a_{11}^2 - 28a_{11}b_{20} - 30a_{20}^2 + 6a_{20}b_{11} + 6b_{11}^2 - 30b_{20}^2)a_{02}$$

$$+ (-10a_{20} + b_{11})a_{11}^2 - 12b_{20}\left(a_{20} + \left(\frac{1}{12}\right)b_{11}\right)a_{11} - (18(a_{20} + (1/2)b_{11}))\left(a_{20}^2 - \left(\frac{4}{3}\right)b_{11}a_{20} + (1/3)b_{11}^2 - \left(\frac{5}{9}\right)b_{20}^2\right)b_{02}$$

$$+ 15a_{02}^3a_{11} + \left(24\left(a_{20} + \left(\frac{3}{8}\right)b_{11}\right)\right)a_{11}a_{02}^2 + \left(\begin{array}{l} 2a_{11}^3 - 7b_{20}a_{11}^2 + (9a_{20}^2 + 9a_{20}b_{11} - 15b_{20}^2)a_{11} \\ + 6b_{11}\left(a_{20} + \left(\frac{1}{2}\right)b_{11}\right)b_{20} \end{array} \right)a_{02}$$

$$+ 2a_{11}^3a_{20} - 8b_{20}\left(a_{20} - \left(\frac{1}{8}\right)b_{11}\right)a_{11}^2$$

$$- \left(10\left(a_{20} + \left(\frac{1}{2}\right)b_{11}\right)\right)b_{20}^2a_{11} + 18b_{11}\left(a_{20} - \left(\frac{1}{3}\right)b_{11}\right)\left(a_{20} + \left(\frac{1}{2}\right)b_{11}\right)b_{20}.$$

(A.1)

For more details of the Lyapunov quantity, see the paper [48] or the expression of L_2 with $\beta = 1$ in the paper [49].

Data Availability

There is no data involved in this paper.

Conflicts of Interest

The authors declare that there is no conflicts of interest regarding the publication of this paper.

Acknowledgments

This study was supported by the National Natural Science Foundation of China (grant nos. 31570364 and 61871293).

References

- [1] S. Ryding and W. Rast, *The Control of Eutrophication of Lakes and Reservoirs*, The Parthenon Publishing Group, Carnforth, Lancashire, UK, 1989.
- [2] F. X. Kong and G. Gao, "Hypothesis on cyanobacteria bloom-forming mechanism in large shallow eutrophic lakes," *Acta Ecologica Sinica*, vol. 25, no. 3, pp. 589–595, 2005.
- [3] A. D. Bazykin, *Nonlinear Dynamics of Interacting Populations*, p. 67, World Scientific, Singapore, 1998.
- [4] A. D. Bazykin, *Structural and Dynamic Stability of Model Predator-Prey Systems*, International Institute for Applied Systems Analysis, Laxenburg, Austria, 1976.
- [5] W. Metzler and W. Wischniewsky, "Bifurcations of equilibria in Bazykin's predator-prey model," *Mathematical Modelling*, vol. 6, no. 2, pp. 111–123, 1985.
- [6] U. Ghosh, S. Pal, and M. Banerjee, "Memory effect on Bazykin's prey-predator model: stability and bifurcation analysis," *Chaos, Solitons & Fractals*, vol. 143, Article ID 110531, 2021.
- [7] P. D. Adhikary, S. Mukherjee, and B. Ghosh, "Bifurcations and hydra effects in Bazykin's predator-prey model," *Theoretical Population Biology*, vol. 140, pp. 44–53, 2021.
- [8] S. Sarwardi, M. Haque, and P. K. Mandal, "Persistence and global stability of Bazykin predator-prey model with Beddington-DeAngelis response function," *Communications in Nonlinear Science and Numerical Simulation*, vol. 19, no. 1, pp. 189–209, 2014.
- [9] P. A. Naik, Z. Eskandari, M. Yavuz, and J. Zu, "Complex dynamics of a discrete-time Bazykin-Berezovskaya prey-predator model with a strong Allee effect," *Journal of Computational and Applied Mathematics*, vol. 413, Article ID 114401, 2022.
- [10] S. T. Wang and H. G. Yu, "Stability and bifurcation analysis of the Bazykin's predator-prey ecosystem with Holling type II," *Mathematical Biosciences and Engineering*, vol. 18, no. 6, pp. 7877–7918, 2021.
- [11] C. S. Holling, "The functional response of predators to prey density and its role in mimicry and population regulation," *Memoirs of the Entomological Society of Canada*, vol. 97, no. S45, pp. 5–60, 1965.
- [12] L. N. Guin and H. Baek, "Comparative analysis between prey-dependent and ratio-dependent predator-prey systems relating to patterning phenomenon," *Mathematics and Computers in Simulation*, vol. 146, pp. 100–117, 2018.
- [13] P. Mishra and S. N. Raw, "Dynamical complexities in a predator-prey system involving teams of two prey and one predator," *Journal of Applied Mathematics and computing*, vol. 61, no. 1-2, pp. 1–24, 2019.
- [14] R. Banerjee, P. Das, and D. Mukherjee, "Stability and permanence of a discrete-time two prey one predator system with Holling type-III functional response," *Chaos, Solitons & Fractals*, vol. 117, pp. 240–248, 2018.
- [15] J. Datta, D. Jana, and R. K. Upadhyay, "Bifurcation and bio-economic analysis of a prey-generalist predator model with Holling type IV functional response and nonlinear age-selective prey harvesting," *Chaos, Solitons & Fractals*, vol. 122, pp. 229–235, 2019.
- [16] D. Mukherjee and C. Maji, "Bifurcation analysis of a Holling type-II predator-prey model with refuge," *Chinese Journal of Physics*, vol. 65, pp. 153–162, 2020.
- [17] L. Perko, *Differential Equations and Dynamical Systems*, Springer-Verlag, New York, NY, USA, 2001.
- [18] Y. Kuznetsov, *Elements of Applied Bifurcation Theory*, pp. 96–100, Springer-Verlag, New York, NY, USA, 2nd edition, 1998.
- [19] J. C. Huang, Y. J. Gong, and J. Chen, "Multiple bifurcations in a predator-prey system of Holling and Leslie type with constant-yield prey harvesting," *International Journal of Bifurcation and Chaos*, vol. 23, no. 10, Article ID 1350164, 2013.
- [20] Z. F. Zhang, T. R. Ding, W. Z. Huang, and Z. X. Dong, *Qualitative Theory of Differential Equations, Transl. Math. Monogr.*, Vol. 101, American Mathematical Society, Providence, RI, 1992.
- [21] L. L. Cai, G. T. Chen, and D. M. Xiao, "Multiparametric bifurcations of an epidemiological model with strong Allee effect," *Journal of Mathematical Biology*, vol. 67, no. 2, pp. 185–215, 2013.
- [22] Y. L. Li and D. M. Xiao, "Bifurcations of a predator-prey system of Holling and Leslie types," *Chaos, Solitons & Fractals*, vol. 34, no. 2, pp. 606–620, 2007.
- [23] D. M. Xiao and S. G. Ruan, "Differential equations with applications to biology: bogdanov-takens bifurcations in predator-prey systems with constant rate harvesting, fields institute communications," *American Mathematical Society*, vol. 21, pp. 493–506, 1999.
- [24] S. N. Chow and J. K. Hale, *Methods of Bifurcation Theory*, Springer-Verlag, New York, NY, USA, 1982.
- [25] R. Bogdanov, "Bifurcations of a limit cycle for a family of vector fields on the plane," *Selecta Mathematica Sovietica*, vol. 1, pp. 373–388, 1981.
- [26] R. Bogdanov, "Versal deformations of a singular point on the plane in the case of zero eigen-values," *Selecta Math.Soviet*, vol. 1, pp. 389–421, 1981.
- [27] F. Takens, "Forced oscillations and bifurcations: applications of global analysis I," *Comm. Math. Inst. Rijksuniv. Utrecht*, vol. 3, pp. 1–59, 1974.
- [28] D. M. Xiao and S. G. Ruan, "Multiple bifurcations in a delayed predator-prey system with n functional response," *Journal of Differential Equations*, vol. 176, no. 2, pp. 494–510, 2001.
- [29] S. N. Chow, C. Z. Li, and D. Wang, *Normal Forms and Bifurcations of Planar Vector fields*, Cambridge University Press, Cambridge, 1994.
- [30] B. Tang and Y. N. Xiao, "Bifurcation analysis of a predator-prey model with anti-predator behaviour," *Chaos, Solitons & Fractals*, vol. 70, pp. 58–68, 2015.
- [31] D. Xiao and K. Fang Zhang, "Multiple bifurcations of a predator-prey system," *Discrete & Continuous Dynamical Systems - B*, vol. 8, no. 2, pp. 417–433, 2007.

- [32] F. Dumortier, R. Roussarie, J. Sotomayor, and K. Zoladek, *Bifurcation of planar vector fields, nilpotent singularities and abelian integrals, Lecture Notes in Math*, vol. 1480, Springer-Verlag, Berlin, 1991.
- [33] J. C. Huang, X. J. Xia, X. N. Zhang, and S. G. Ruan, “Bifurcation of codimension 3 in a predator-prey system of Leslie type with simplified Holling type IV functional response,” *International Journal of Bifurcation and Chaos*, vol. 26, no. 02, Article ID 1650034, 2016.
- [34] J. Gine, “On some open problems in planar differential systems and Hilbert’s 16th problem,” *Chaos, Solitons & Fractals*, vol. 31, no. 5, pp. 1118–1134, 2007.
- [35] V. A. Gaiko, “Wintner-Perko termination principle, parameters rotating a field, and limit-cycle problem,” *Journal of Mathematical Sciences*, vol. 126, no. 4, pp. 1259–1266, 2005.
- [36] V. A. Gaiko, “Global bifurcation analysis of a rational Holling system,” *Computer Research and Modeling*, vol. 9, no. 4, pp. 537–545, 2017.
- [37] X. X. Qiu and H. B. Xiao, “Qualitative analysis of Holling type II predator-prey systems with prey refuges and predator restraints,” *Nonlinear Analysis: Real World Applications*, vol. 14, no. 4, pp. 1896–1906, 2013.
- [38] W. Yuquan, J. Zhujun, and K. Y. Chan, “Multiple limit cycles and global stability in predator prey model,” *Acta Mathematicae Applicatae Sinica*, vol. 15, no. 2, pp. 206–219, 1999.
- [39] J. Alidousti, “Stability and bifurcation analysis for a fractional prey-predator scavenger model,” *Applied Mathematical Modelling*, vol. 81, pp. 342–355, 2020.
- [40] B. Dubey, A. Kumar, and A. Patra Maiti, “Global stability and Hopf-bifurcation of prey-predator system with two discrete delays including habitat complexity and prey refuge,” *Communications in Nonlinear Science and Numerical Simulation*, vol. 67, pp. 528–554, 2019.
- [41] Y. Lv, Y. Z. Pei, and Y. Wang, “Bifurcations and simulations of two predator-prey models with nonlinear harvesting,” *Chaos, Solitons & Fractals*, vol. 120, pp. 158–170, 2019.
- [42] M. Sambath, K. Balachandran, and L. N. Guin, “Spatiotemporal patterns in a predator-prey model with cross-diffusion effect,” *International Journal of Bifurcation and Chaos*, vol. 28, no. 02, pp. 1830004–1830012, 2018.
- [43] L. N. Guin, B. Mondal, and S. Chakravarty, “Cross-diffusion-driven pattern formation and selection in a modified Leslie-Gower predator-prey model with fear effect,” *Journal of Biological Systems*, vol. 28, no. 1, pp. 1–38, 2020.
- [44] L. N. Guin, E. Das, and M. Sambath, “Pattern formation scenario through Turing instability in interacting reaction diffusion systems with both refuge and nonlinear harvesting,” *Journal of Applied Nonlinear Dynamics*, vol. 9, no. 1, pp. 1–21, 2020.
- [45] X. X. Li, H. G. Yu, C. J. Dai, Z. L. Ma, Q. Wang, and M. Zhao, “Bifurcation analysis of a new aquatic ecological model with aggregation effect,” *Mathematics and Computers in Simulation*, vol. 190, pp. 75–96, 2021.
- [46] V. Tiwari, J. P. Tripathi, R. K. Upadhyay, Y. P. Wu, J. S. Wang, and G. Q. Sun, “Predator-prey interaction system with mutually interfering predator: role of feedback control,” *Applied Mathematical Modelling*, vol. 87, pp. 222–244, 2020.
- [47] D. Jusufovski and A. Kuparinen, “Exploring individual and population eco-evolutionary feedbacks under the coupled effects of fishing and predation,” *Fisheries Research*, vol. 231, Article ID 105713, 2020.
- [48] N. Serebryakova, “Behavior of dynamical system with one degree of freedom near the points of boundaries of domain of stability, where a safe boundary goes to the dangerous one (in Russian),” *Mechanics and Engineering*, vol. 2, pp. 178–182, Division of Technical Sciences, 1959.
- [49] N. V. Kuznetsov and G. A. Leonov, “Computation of Lyapunov quantities,” in *Proceedings of the 6th EUROMECH Nonlinear Dynamics Conference (ENOC 2008)*, Saint Petersburg, Russia, July 2008.